# The hybrid vehicle-drone routing problem for pick-up and delivery services

Aline Karak, Khaled Abdelghany*

*Department of Civil and Environmental Engineering, Southern Methodist University, P.O. Box 750340, Dallas, TX 75275-0340, United States*

ARTICLE INFO

ABSTRACT

This paper presents a mathematical formulation and efficient solution methodology for the hybrid vehicle-drone routing problem (HVDRP) for pick-up and delivery services. The problem is formulated as a mixed-integer program, which minimizes the vehicle and drone routing cost to serve all customers. The formulation captures the vehicle-drone routing interactions during the drone dispatching and collection processes and accounts for drone operation constraints related to flight range and load carrying capacity limitations. A novel solution methodology is developed which extends the classic Clarke and Wright algorithm to solve the HVDRP. The performance of the developed heuristic is benchmarked against two other heuristics, namely, the vehicle-driven routing heuristic and the drone-driven routing heuristic. A set of experiments are conducted to evaluate the performance of the developed heuristics and to illustrate the capability of the developed model in answering a wide variety of questions related to the planning of the vehicle-drone delivery system.

## 1. Introduction

The evolution of drone technology during the past decade has opened the door for numerous innovative applications in transportation/logistics (Troudi et al., 2017; Kunze, 2016; Menouar et al., 2017), defense (Paust, 2010; Schneiderman, 2012), public safety and security (Chowdhury et al., 2017; Clarke and Moses, 2014; Vattapparamban et al., 2016; Merwaday and Guvenc, 2015), healthcare (Thiels et al., 2015; Kim et al., 2017; Balasingam, 2017), and forestry and agriculture (Getzin et al., 2012), to name a few. In particular, the use of drones for product delivery has received considerable attention following Amazon's recently announced plan to use drones for product delivery (Rose, 2013). A leading U.S. delivery company estimates an annual cost saving of about $50 M if drones replaced its trucks for the last mile of the delivery trip (Rash, 2017). Drone usage for delivery applications is expected to grow significantly in the next few years. Several contributing factors to this growth include: (1) the expanding online retail industry; (2) improved capability, reliability, and cost effectiveness of drones; and (3) high competition among pick-up and delivery service providers. Therefore, there are increasing calls to develop innovative pick-up and delivery systems that integrate drones in order to meet growing demand and reduce service costs.

Effort is underway to develop a technology that meets the requirements of product delivery applications. Drone manufacturers are developing the next-generation drones with increased travel ranges, load carrying capacity, positioning accuracy, durability, and battery charging rates (Floreano and Wood, 2015). A parallel effort is devoted to studying the logistical aspects of adopting drones for delivery services, taking into consideration regulatory rules and operational constraints. For example, flying side-kick system, in

---

* Corresponding author.
*E-mail addresses:* akarak@smu.edu (A. Karak), khaled@smu.edu (K. Abdelghany).

which one drone is mounted on the vehicle and used to visit selected customers, has been developed to address these logistical constraints (Murray and Chu, 2015). However, this system does not take full advantage of drone capabilities in terms of visiting multiple customer per dispatch and possibilities for more efficient vehicle-drone integration.

In this context, a novel system recently conceptualized for using drones to provide product delivery services is the integrated vehicle-drone system (a.k.a. the "mothership" system). The system generally consists of vehicles (trucks or vans) that carry unmanned vehicles (robots and/or drones) from their depots to neighborhoods where the unmanned vehicles are dispatched to perform multiple pick-up and delivery tasks (McFarland, 2016). Different from the flying side-kick system, the mothership system adopts a "swarm" dispatching approach, which allows dozens of pick-ups and deliveries to be performed simultaneously (PYMNTS, 2016; Petersen, 2016). Such a system is estimated to double the average number of packages delivered in a typical working shift as compared to the conventional system in which a vehicle completes one delivery at a time (Lockridge, 2017). The mothership system can be viewed as a version of the pick-up and delivery problem, which can be classified into three different problem categories: one-to-one, one-to-many-to-one, and many-to-many (Berbeglia et al., 2010). In the one-to-one problem, each commodity is transported directly from an origin to a destination. In the one-to-many-to-one problem, commodities are transported from a single depot to customers, and commodities picked from the customers are transported to that depot. Finally, the many-to-many problem involves transporting commodities from multiple depots to multiple customers, and vice versa. The mothership system studied in this paper is a one-to-many-to-one problem, as the vehicle and the drones are dispatched from one depot to deliver commodities to customers, and pick-up commodities from the customers and transport them back to the depot.

Integrating drones with a vehicle in the form of the mothership system presents several advantages as compared to previously proposed systems such as the flying side-kick delivery system. For example, the mothership system considers the dispatching of multiple drones simultaneously, and each drone can serve multiple customers per dispatch. On the other hand, the side-kick system assumes that only one drone is used, which serves one customer per dispatch. Furthermore, the mothership system offers flexibility in terms of the drone dispatching and collection locations (i.e., these could be the same or different). The side-kick system forces the drone collection location to be different from its dispatching location, as the vehicle does not wait at the dispatching location. Also, in the side-kick system, drones are used for package delivery only without the option to provide package pick-up services along their tours. Thus, the superior and flexible configuration of the mothership system provides the capability to perform pick-up and delivery services more efficiently. The mothership system is also envisioned to reduce congestion caused by trucking in urban areas as it increases dependence on drones and reduces the number of required vehicle stops as compared to the side-kick system, where most customers are served by the vehicle. In addition, the mothership system is expected to reduce the workload on the driver as it limits her/his tasks to driving between specified stops and loading/unloading packages from the drones. Thus, the driver is not involved in any door-to-door pick-up or delivery tasks, which enhances her/his working conditions and safety. Finally, while the side-kick system assumes that drone dispatches and collections occur at a customer location, the mothership system allows the vehicle to dispatch and collect the drones at special locations that can be sensibly selected to limit any inconvenience (e.g., noise, safety, and aesthetic) to the customers.

Designing a hybrid vehicle-drone system for pick-up and delivery services entails determining the optimal setting of several system parameters including: (a) vehicle and drone resources required for the pick-up and delivery tasks; (b) locations (stations) for drone dispatching and collection; (c) tactics used to dispatch and collect the drones; (d) number of customers visited per drone dispatch; and (e) optimal vehicle and drone routing decisions. For example, the number of vehicles, the number of drones mounted on each vehicle, and the capabilities of the drones in terms of their flying ranges and load carrying capacities should be determined for each operation. The locations for dispatching and collecting the drones should be selected to ensure that all customers can be reached by the drones. Furthermore, two tactics may be considered for drone dispatching and collection. First, a vehicle could dispatch its drone(s) at a location and wait at the same location to collect the drone(s). This dispatch-wait-collect tactic is suitable in cases where drones must remain within sight for safety considerations. Alternatively, the dispatch-move-collect tactic allows the vehicle to move after dispatching the drones. The drones could be collected at another location by the same vehicle or by another available vehicle. Finally, the optimal route for each drone should be determined in terms of its dispatching and collection stations and the sequence of customers visited. Optimal vehicle routes should be determined in terms of the sequence of customers to be served, if any, and the sequence of stations used for drone dispatching and collection.

Several sources of complexity characterize the hybrid vehicle-drone routing problem (HVDRP). First, even for small size problems, the HVDRP involves a large number of decision variables including vehicle and drone resources/capabilities, locations of drone dispatching and collection, and routing decisions for the vehicles and the drones. The problem can be generally viewed as an extension of the classic vehicle routing problem (VRP) which is known to be an NP-hard problem (Golden et al., 2008). Thus, the execution time required to obtain an exact optimal solution grows exponentially as the problem size increases. Second, most decision variables involved in this problem are highly interdependent and cannot be optimized separately. For example, the locations for drone dispatching and collection depend on the drone's flying range and load carrying capabilities, and vice versa. Furthermore, optimizing vehicle routes and drone routes independently could result in a sub-optimal solution, because the vehicle routes determine the stations for dispatching and collecting the drones, which in turn define the origins and destinations of the drones' routes. The locations of the dispatch and collection stations are simultaneously impacted by the sequence of customers visited by the drones. Finally, because such a system has not yet been deployed in the real-world, developing a model to study the HVDRP requires making several assumptions related to defining the configuration of the system and its operational parameters.

A mathematical formulation in the form of a mixed-integer program (MIP) is developed for the problem. The formulation solves for the optimal drone and vehicle routes to serve all customers such that the total cost of the pick-up and the delivery operation is minimized. The formulation considers operational constraints for the vehicle and drones and captures their interdependence. Due to the NP-hard nature of the HVDRP, its optimal solution can only be obtained in a reasonable execution time for small problem

instances. Thus, there is a need to develop efficient heuristics that can be used to obtain a good solution for large problem instances such as those anticipated in real-world applications. To achieve this goal, we introduce a novel solution methodology that extends the classic Clarke and Wright algorithm, the hybrid Clarke and Wright heuristic (HCWH) (Clarke and Wright, 1964). The heuristic considers the cost savings for both the vehicle and the drones while solving for the optimal vehicle route, thus generating an efficient multimodal vehicle-drone network. The performance of the HCWH is benchmarked against two other heuristics that are developed as part of this research, which are the vehicle-driven heuristic (VDH) and the drone-driven heuristic (DDH). In the VDH, the optimal vehicle route is obtained first and then the drones are routed, assuming a fixed vehicle route. A reverse approach is considered for the DDH: given the optimal drone routes, the vehicle is routed to enable the dispatching and collection of the drones. The performance of these heuristics is compared in terms of the solution quality and the required execution time considering several randomly generated networks of different sizes and configurations.

This paper contributes to the existing literature in several ways. First, to the authors' knowledge, this paper is among the first to develop a model to study the mothership system at a high realism. Most existing models fall short of representing the drones' capabilities in terms of flight range and load carrying capacity, and consequently, misrepresent their impact on routing decisions. Moreover, this model considers advanced features for the HVDRP that are technically feasible and could result in significant cost savings, such as allowing the drones to visit multiple customers in a single dispatch and allowing them to be dispatched and collected at two different locations. Second, the paper presents a comprehensive mathematical formulation that can be used to obtain the optimal solution for small size problems in order to benchmark the solution quality of the developed heuristics. The formulation considers the main operational constraints defined for the problem including interdependence between the vehicle and the drones and the limitations of the drones in terms of flight range and load carrying capacity. Third, we present a novel extension of the classic Clarke and Wright algorithm to solve the HVDRP. The cost savings computed at each iteration account for both vehicle and drone routing costs. Thus, the solution simultaneously optimizes the routing decisions for the multimodal vehicle-drone network. Finally, the paper presents a sensitivity analysis to examine the effect of several system parameters on the overall performance of the network.

This paper is organized as follows. Section 2 presents a review of previous models developed for studying the integrated vehicle-drone routing problem. Section 3 provides a formal definition of the problem and Section 4 presents the problem's mathematical formulation. Section 5 presents the hybrid Clarke and Wright heuristic along with the vehicle-driven and drone-driven heuristics. Section 6 describes the experiments designed to evaluate the developed solution methodologies and analyzes their results. Finally, Section 7 provides concluding remarks and presents possible research extensions.

## 2. Literature review

As mentioned earlier, the HVDRP can be viewed as a generalization of the classical vehicle routing problem (VRP) in which a vehicle uses the shortest route to visit several customers and returns back to its depot. A summary of common versions of the VRP, their formulations, and their solution methodologies can be found in Golden et al. (2008, Eksioglu et al. (2009), and Braekers et al. (2014). While limited work is devoted to studying the HVDRP, several versions of the classical VRP share features of the HVDRP. For example, the green vehicle routing problem (GVRP) presented by Erdogan and Miller-Hooks (2012), Schneider et al. (2014), and Hiermann et al. (2016) entails scheduling efficient routes for electric vehicles that are required to stop at charging stations distributed in the network to recharge their batteries. Failing to schedule proper stops for battery recharging precludes the vehicles from completing their scheduled tour and/or returning to their depots. As such, scheduling stops for battery recharging is a hard constraint for the vehicles in the GVRP. A similar constraint should be considered for the drones in the HVDRP as their batteries need to be recharged in order to complete their tours. In addition, the HVDRP is similar to the capacitated vehicle routing problem (CVRP), where each vehicle has a limited carrying capacity (Christofides, 1976, Fukasawa et al., 2006, Xiao et al., 2012, and Borcinova, 2017). As each drone has limited flight range and load carrying capacity, the HVDRP naturally extends the CVRP.

The two-echelon location and routing problem (2E-LRP) also shares similarities with the HVDRP (Nguyen et al., 2012; Govindan et al., 2014; Cuda et al., 2015). The problem considers two level trips. The upper-level trips are performed by large vehicles that start from the main depot to distribute goods to a set of satellite depots and return to the main depot. The lower-level trips are performed by small vehicles serving the end customers. These trips start and end at the satellite depots. Although both the 2E-LRP and the HVDRP involve two-level routing, these two-level routing decisions are independent in the 2E-LRP and are fully interdependent in the HVDRP. The routes for the two vehicle types in the 2E-LRP can be determined separately, while the HVDRP requires coordinating the routing decisions of the vehicle and the drones as any change in the vehicle route might affect the drone routes, and vice versa.

Another similar problem is the truck and trailer routing problem (TTRP) which requires a subset of customers to be visited by a truck-trailer pair, while other customers are visited by the truck alone (e.g., Chao, 2002; Lin et al., 2009; Derigs et al., 2013; Villegas et al., 2013). The TTRP is similar to the HVDRP in the sense that both problems require routing two types of vehicles. The TTRP integrates the truck and the trailer, while the HVDRP integrates the vehicle and the drone. Nonetheless, while the drone moves independently without the vehicle, a trailer can only be moved by connecting it to a truck. Lin (2011) presented another multimodal routing problem that considers cooperation between heavy resources (truck) and a light resource (scooter) to serve customers within a certain time window. The truck carries the scooter which can disembark from the truck to serve the customers independently. The problem assumes that each scooter disembarks only once while the truck must wait for its return.

Drone routing research increased over the past few years. For example, Shetty et al. (2008) considered a problem in which a fleet of drones is routed to serve a set of predetermined locations with different priorities. The drone routes are constrained by their flight range and payload capacity. A modeling framework is developed which decomposes the problem into a target assignment problem and a vehicle routing problem. A solution methodology that adopts a tabu search heuristic is developed to coordinate both problems.

Avellar et al. (2015) developed an optimization model for a minimum time area coverage using a fleet of drones taking into consideration the maximum flight time and the setup time. The number of drones used is chosen as a function of the size and the format of the area. The framework assumed that each drone can be used only once, ignoring the possibility of re-dispatching after battery recharging. The work of Grochlsky et al. (2006) and Fargeas et al. (2015) focused on surveillance applications in which drones equipped with sensors cooperate with an unmanned a ground vehicle (UAG) to accurately locate ground target. Dorling et al. (2016) are among the first to study the drones delivery problem (DDP). A model is proposed which constructs drone routes that account for battery and payload weight limitations and allow for multiple deliveries per route. However, all drones are assumed to be dispatched and collected at a single depot. These problems do not consider the mothership model, and hence are essentially solved as a classical vehicle routing problem with capacity constraints.

Research that takes into consideration vehicle-drone integration for delivery services is still in its infancy. Murray and Chu (2015) introduced the flying sidekick traveling salesman problem (FSTSP) and the parallel drone scheduling TSP (PDSTSP) that aim to minimize the total travel time of the truck and the drone. They proposed two MIPs formulation and two simple heuristics that were tested on small problem instances of up to 10 customers. Agatz et al. (2016) studied a similar problem to the FSTSP called the traveling salesman problem with drone (TSP-D). They provided an MIP which was solved using the truck-first-drone-second heuristic. The heuristic implements dynamic programming and local search techniques to determine efficient drone routes. Bouman et al. (2017) proposed an exact approach for the TSP-D based on dynamic programing, which was shown to solve larger instances. Furthermore, Wang et al. (2017) introduced a more general problem called the vehicle routing problem with drone (VRP-D) that considers multiple trucks and drones with the objective of minimizing the total duration of the delivery mission. While no optimization framework is provided for the problem, the work focused on testing several worst-case scenarios to develop bounds on the best possible time savings for truck-drone integration compared to the truck-alone case. Each drone is assigned multiple customers per dispatch and the drone is set to return to its dispatching truck, which waits for the drone at the dispatching location. The work was later extended by Poikonen et al. (2017) to consider limitation of the drones' battery life and extend the worst-case bounds to a more generic distance/cost matrix. Finally, in a more recent work, Ha et al. (2018) built on the FSTSP presented in Murray and Chu (2015), but instead of minimizing the delivery completion time, they minimized the total operation cost. The problem is also formulated in the form of an MIP which was solved using a heuristic that adopts greedy randomized adaptive search procedure (GRASP). Extending the PDSTSP presented by Murray and Chu (2015), Ham (2018) developed a constraint programming method to solve a problem in which multiple vehicles and multiple drones perform pick-up and delivery services. Kim and Moon (2019) extended the same problem, considering a single vehicle and multiple drones, to allow the drones to be dispatched, independently from the vehicle, from the depot as well as from pre-specified customer locations. They provided an MIP that was solved through an efficient decomposition approach. Jeong et al. (2019) extended the FSTSP to consider the energy consumption of drones and restricted flying areas. An MIP is presented along with a two-phase constructive and search heuristic that is used to solve real world instances.

To the authors' knowledge, models that consider full vehicle-drone routing integration in the form of a mothership system have not been developed. Most existing models focus on using the drones in the form of flying side-kick system. In addition, these models are limited in terms of representing the main features and operational constraints that characterize the integrated vehicle-drone routing problem. For example, they force certain routes for the drones (e.g., drones are prohibited for returning to their dispatch locations for collection) and they force a certain strategy for drone dispatch and collection (e.g., either the dispatch-wait-collect or the dispatch-move-collect, but not both). In addition, they fall short of representing the operational limitations of the drones in terms of flight range and load carrying capacity in the context of the mothership delivery system. They also limit the drone usage for package delivery only for a pre-determined set of customers without the option to provide package pick-up services along their tours. Finally, existing models assume a homogenous drone fleet in terms of operation cost, flight range, and load carrying capacity, which might not be the case in real-world applications.

## 3. The hybrid vehicle-drone routing problem

This section defines the HVDRP for pick-up and delivery services. The following assumptions are considered, which specify the operation scenarios of the proposed mothership system:

1. Multiple drones are mounted on a single vehicle.
2. Each drone can serve more than one customer per dispatch as long as its flight range and load carrying capacity are not violated.
3. Drones can return to any station along the vehicle route, which could be the same as or different from the dispatching one.
4. Multiple drones can be dispatched simultaneously from any station, which allows the use of a swarm of drones to enhance the overall productivity of the system.
5. Each station can be visited by the vehicle only once.
6. Customers are served only by drones.
7. Vehicles are used only as mobile depots for the drones in order to reduce the required number of vehicle stops.
8. Drones can be dispatched and collected several times from the same station.
9. The vehicle cannot move from a station before collecting all drones that are planned to return to that station.
10. Drones that arrive to a collection station early are assumed to wait for the vehicle in idle conditions before being assigned a new tour. This assumption in conjunction with assumption 9, ensures a proper visitation sequence for the vehicle and the drones.
11. Drone batteries are replaced with fully charged batteries each time they are collected by the vehicle.
12. Packages are loaded and unloaded from the drones once the drones have been collected by the vehicle.

Each drone is defined in terms of its maximum flying range and load carrying limitation. The vehicle starts and ends its route at a depot and stops at selected stations to dispatch and/or collect the drones. The stations are locations where the vehicle and drones may wait for each other for collection. This configuration allows the vehicle to accommodate multiple dispatches of the same drone from a certain station to serve a dense customer population around that station. As the system involves multiple drones, these drones are expected to arrive at their collection stations at different times. Drones that arrive early wait in idle condition until the vehicle arrives. At any of these stations, drones could be dispatched such that each drone visits one or more customers to pick-up and/or deliver their packages. Each package is defined in terms of its weight. The drone route must ensure that its maximum flying range and load carrying capacity are not violated. A drone may return to any station along the vehicle's route for collection. After battery replacement and package loading/unloading, the drone can be dispatched again to serve a new set of customers. The process is repeated until all customers in the service area have been reached. This configuration takes advantage of the expected reduced drone operation cost, compared to the vehicle cost, and provides more flexibility in routing the drones and the vehicle. Thus, the system is able to provide efficient integration between the vehicle and the drones to reduce dependence on the vehicle and increase the use of drones in performing the pick-up and delivery services. The resulting system is expected to reduce the total system operation cost, alleviate congestion associated with urban trucking, and enhance the drivers' work conditions. The following notations describe data sets, model parameters, and decision variables used to formulate the HVDRP.

Notations:

Sets:
| | |
|---|---|
| $G$ | Directed multimodal network |
| $N$ | Set of nodes, indexed by $i, j, k, l, m$ and $n \in N$ |
| $N_D$ | Subset that includes the depot node |
| $N_V$ | Subset of station nodes |
| $N_C$ | Subset of customer nodes |
| $N_1$ | Subset of nodes accessible by the vehicle ($N_D \cup N_V$) |
| $A$ | Set of links, index by node pair $(i, j)$, where $i \in N$ and $j \in N$ |
| $D$ | Set of drones, indexed by $d \in D$ |

Parameters:
| | |
|---|---|
| $q_m$ | Delivery weight of customer located at node $m \in N_C$ |
| $p_m$ | Pickup weight of customer located at node $m \in N_C$ |
| $r_d$ | Maximum flight range of drone $d \in D$ |
| $w_d$ | Load lifting capacity of drone $d \in D$ |
| $l_{ij}$ | The length of link $(i, j) \in A$ |
| $cv_{ij}$ | Average travel cost from node $i \in N_1$ to $j \in N_1$ for the vehicle |
| $cd_{ij}^d$ | Average travel cost from node $i \in N$ to $j \in N$ for drone $d \in D$ |
| $M1$ | Very large positive number – the maximum possible distance travelled by the vehicle. One possible value for $M1$ is the vehicle traveled distance obtained using the drone-driven heuristic (DDH) as it provides a good upper bound on the vehicle traveled distance. |
| $M2$ | Very large positive number – the maximum possible load carrying capacity by a drone |
| $M2$ | $= \max (w_d \ \forall \ d \in D)$ |
| $M3$ | Very large positive number – the maximum possible flight range by a drone |
| $M3$ | $= \max (r_d \ \forall \ d \in D)$ |

Decision variables:
| | |
|---|---|
| $x_{dij}$ | $= 1$ if drone $d \in D$ traverses link $(i, j) \in A$ on-board of the vehicle, and 0 otherwise |
| $y_{ij}$ | $= 1$ if the vehicle traverses link $(i, j) \in A$, and 0 otherwise |
| $z_{jdml}$ | $= 1$ if drone $d \in D$ dispatched from station $j \in N_V$ travels on link $(m, l) \in A$, and 0 otherwise |
| $b_{ijd}$ | $= 1$ if drone $d \in D$ dispatched from station $j \in N_V$ is collected at station $i \in N_V$, and 0 otherwise |
| $f_{jd}$ | $= 1$ if drone $d \in D$ is dispatched from station $j \in N_V$, and 0 otherwise |
| $dw_{ijd}$ | $=$ Delivery load carried by drone $d \in D$ after visiting node $i \in N$ and heading to node $j \in N$ |
| $pw_{ijd}$ | $=$ Pick-up load carried by drone $d \in D$ after visiting node $i \in N$ and heading to node $j \in N$ |
| $dst_{ijd}$ | $=$ Remaining flight range of drone $d \in D$ after visiting node $i \in N$ and heading to node $j \in N$ |
| $u_i$ | $=$ Specifies the order of node $i \in N_1$ in the vehicle route |
| $d_{ij}$ | $=$ Total distance traveled by the vehicle after traveling on link $(i, j) \in A$ |

Consider a multimodal vehicle-drone network $G(N, A)$, where $N$ is the set of nodes and $A$ is the set of links. A set of drones $D$ mounted on a vehicle are assumed to provide pick-up and delivery services for customers distributed in this network. The vehicle starts and ends its tour at a single depot. The set of nodes $N = N_D \cup N_V \cup N_C$ includes the depot node in $N_D = \{0\}$, the station nodes $N_V = \{1, 2, \cdots, |N_V|\}$ where the vehicle can stop to dispatch and collect the drones, and the customer nodes $N_C = \{|N_V| + 1, \cdots, |N_V| + |N_C|\}$. Thus, $N_1 = N_D \cup N_V$ represents the subset of nodes that can be reached by the vehicle, while the subset $N_C$ includes nodes that are accessible only by the drones. The pick-up weight, $p_m$, and the delivery weight, $q_m$, are assumed to be given for each customer node $m \in N_C$. Each link, $(i, j) \in A$, is defined in terms of its length, $l_{ij}$, the average travel cost by the vehicle, $cv_{ij}$, and the average travel cost by each drone, $cd_{ij}^d$. These costs are assumed to be a function of the length of the link $(i, j)$ and the cost per unit distance for each mode. The travel cost per unit distance for all drones is assumed to be less than that of the vehicle. Each drone, $d \in D$, is defined in terms of its maximum load carrying capacity, $w_d$, and maximum flight range, $r_d$, which depends on its battery lifespan. A drone cannot exceed its maximum flight range or its maximum carrying load. Customers are served by drones that are dispatched and collected by the vehicle at certain stations. The problem requires determining the optimal route for the vehicle

and the drones such that all customers in the network are served with the minimum total travel cost for the vehicle and the drones.

Several decision variables are defined for this problem. To represent the vehicle route, we define $y_{ij} \in \{0, 1\}$, which is equal to one if the vehicle travels on link $(i, j) \in A$, and zero otherwise. The variable $x_{dij} \in \{0, 1\}$ is equal to one if drone $d \in D$ is mounted on the vehicle while traveling on link $(i, j) \in A$, and zero otherwise. The drone route is defined by the binary variable $z_{jdlm} \in \{0, 1\}$, which is equal to one if drone $d \in D$ dispatched from node $j \in N_V$ travels on link $(l, m) \in A$, and zero otherwise. The delivery and pick-up load carried by drone $d \in D$ after departing from node $i \in N$ and heading to node $j \in N$ is given by $dw_{ijd} \geq 0$ and $pw_{ijd} \geq 0$, respectively. The variable $dst_{ijd} \geq 0$ defines the remaining flight range of drone $d \in D$ after traveling link $(i, j) \in A$ and heading to node $j \in N$. This decision variable is used to determine if the drone has the adequate flight range to travel link $(i, j) \in A$. Additional variables are also used to define the vehicle-drone interaction. We define the variable $f_{jd} \in \{0, 1\}$, which is equal to one if drone $d \in D$ is dispatched from the vehicle at node $j \in N_V$. Also, the variable $b_{ijd} \in \{0, 1\}$ is equal to one if drone $d \in D$ that is dispatched at node $j \in N_V$ is collected by the vehicle at node $i \in N_V$. To track the vehicle's traveled distance, we introduce the variable $d_{ij}$, which is defined as the total distance traveled by the vehicle after traveling on link $(i, j) \in A$. Finally, the variable $u_i$ is used to ensure subtour elimination for the vehicle such that $1 \leq u_i \leq |N_V| + 1$.

## 4. Mathematical formulation

This section presents the mathematical formulation developed for the HVDRP. This formulation presents a first attempt to model the mothership system. While the formulation presents a set of variables and constraints that capture the unique aspects of the problem, it also takes advantage of the similarities that exist between the HVDRP with the TTRP and CVRP. For example, it extends the TTRP to represent the vehicle transportation of the drones along the different links by using variables $y_{ij}$ and $x_{dij}$, which describe the movement of the vehicle and any mounted drones. It also borrows features from existing formulations of the CVRP such as variables $dw_{ijd}$, $pw_{ijd}$, and $dst_{ijd}$ that track the drones' load carrying capacity and flying range. In addition, a new dimension is added to the decision variable used to describe the drone (i.e., capacitated vehicles) routing decisions, $z_{jdlm}$, in order to match the drones with their dispatching stations and hence capture the vehicle-drone interactions aspect of the problem.

The problem is modeled in the form of an MIP as presented below. Considering an objective function that minimizes the total operation cost for the vehicle and the drones, four main sets of constraints are defined as follows:

- Depot constraints,
- Vehicle constraints,
- Drone constraints, and
- Vehicle-drone interaction constraints.

The expression in (1) and Eqs. (2)–(43) describe the MIP for the HVDRP.

Objective function:

$$\text{Minimize} \sum_{i \in N_1} \sum_{j \in N_1} y_{ij} \cdot cv_{ij} + \sum_{j \in N_v} \sum_{d \in D} \sum_{m \in N} \sum_{l \in N} z_{jdml} \cdot cd^d_{ml} \tag{1}$$

Depot constraints:

$$\sum_{j \in N_v} y_{kj} = 1 \quad \forall \, k \in N_D \tag{2}$$

$$\sum_{j \in N_v} y_{jk} = 1 \quad \forall \, k \in N_D \tag{3}$$

$$\sum_{j \in N_v} \sum_{d \in D} \sum_{k \in N_D} x_{dkj} = \sum_{j \in N_v} \sum_{d \in D} \sum_{k \in N_D} x_{djk} \tag{4}$$

Vehicle constraints:

$$\sum_{\substack{j \in N_1 \\ j \neq i}} y_{ij} = \sum_{\substack{j \in N_1 \\ j \neq i}} y_{ji} \quad \forall \, i \in N_1 \tag{5}$$

$$d_{ki} \leq l_{ki} + M1 \times (1 - y_{ki}) \quad \forall \, i \in N_1, \forall \, k \in N_D \tag{6}$$

$$d_{ki} \geq l_{ki} - M1 \times (1 - y_{ki}) \quad \forall \, i \in N_1, \forall \, k \in N_D \tag{7}$$

$$d_{ij} \leq d_{ki} + l_{ij} + M1 \times (2 - y_{ij} - y_{ki}) \quad \forall \, i \in N_V, \forall \, j \in \{N_1 : j \neq i\}, \forall \, k \in \{N_1 : k \neq i\} \tag{8}$$

$$d_{ij} \geq d_{ki} + l_{ij} - M1 \times (2 - y_{ij} - y_{ki}) \quad \forall \, i \in N_V, \forall \, j \in \{N_1 : j \neq i\}, \forall \, k \in \{N_1 : k \neq i\} \tag{9}$$

$$d_{ij} \leq M1 \times y_{ij} \quad \forall \, i \in N_1, \forall \, j \in N_1 \tag{10}$$

Drone constraints:

$$z_{jdlm} \leq \sum_{k \in N_C} z_{jdjk} \qquad \forall\, d \in D,\, \forall\, l \in N,\, \forall\, m \in N,\, \forall\, j \in N_V \tag{11}$$

$$z_{jdik} = 0 \qquad \forall\, d \in D,\, \forall\, k \in N,\, \forall\, i \in N_1,\, \forall\, j \in \{N_V: j \neq i\} \tag{12}$$

$$\sum_{j \in N_v} \sum_{d \in D} \sum_{l \in N} z_{jdlm} = 1 \qquad \forall\, m \in N_C \tag{13}$$

$$\sum_{\substack{l \in N \\ l \neq m}} z_{jdlm} = \sum_{\substack{n \in N \\ n \neq m}} z_{jdmn} \qquad \forall\, d \in D,\, \forall\, m \in N_C,\, \forall\, j \in N_V \tag{14}$$

$$dw_{ikd} + pw_{ikd} \leq w_d \qquad \forall\, d \in D,\, \forall\, i \in N,\, \forall\, k \in N \tag{15}$$

$$\sum_{k \in N} pw_{jkd} = M2 \times (1 - z_{jdjm}) \qquad \forall\, d \in D,\, \forall\, j \in N_V,\, \forall\, m \in N_C \tag{16}$$

$$dw_{mkd} \geq dw_{lmd} - q_m - M2 \times (2 - z_{jdlm} - z_{jdmk}) \qquad \forall\, d \in D,\, \forall\, j \in N_V,\, \forall\, m \in \{N_C: m \neq j\},\, \forall\, l \in \{N: l \neq m\},\, \forall\, k \in \{N: k \neq m\} \tag{17}$$

$$dw_{mkd} \leq dw_{lmd} - q_m + M2 \times (2 - z_{jdlm} - z_{jdmk}) \qquad \forall\, d \in D,\, \forall\, j \in N_V,\, \forall\, m \in \{N_C: m \neq j\},\, \forall\, l \in \{N: l \neq m\},\, \forall\, k \in \{N: k \neq m\} \tag{18}$$

$$pw_{mkd} \geq pw_{lmd} + p_m - M2 \times (2 - z_{jdlm} - z_{jdmk}) \qquad \forall\, d \in D,\, \forall\, j \in N_V,\, \forall\, m \in \{N_C: m \neq j\},\, \forall\, l \in \{N: l \neq m\},\, \forall\, k \in \{N: k \neq m\} \tag{19}$$

$$pw_{mkd} \leq pw_{lmd} + p_m + M2 \times (2 - z_{jdlm} - z_{jdmk}) \qquad \forall\, d \in D,\, \forall\, j \in N_V,\, \forall\, m \in \{N_C: m \neq j\},\, \forall\, l \in \{N: l \neq m\},\, \forall\, k \in \{N: k \neq m\} \tag{20}$$

$$dw_{lmd} \leq \sum_{j \in N_v} M2 \times z_{jdlm} \qquad \forall\, d \in D,\, \forall\, l \in N,\, \forall\, m \in N \tag{21}$$

$$pw_{lmd} \leq \sum_{j \in N_v} M2 \times Z_{jdlm} \qquad \forall\, d \in D,\, \forall\, l \in N,\, \forall\, m \in N \tag{22}$$

$$dst_{jkd} = r_d \times z_{jdjk} \qquad \forall\, d \in D,\, \forall\, j \in N_V,\, \forall\, k \in N \tag{23}$$

$$dst_{ikd} \geq l_{ik} \times z_{jdik} \qquad \forall\, d \in D,\, \forall\, j \in N_V,\, \forall\, (i, k) \in A \tag{24}$$

$$dst_{mkd} \geq dst_{lmd} - l_{lm} - M3 \times (2 - z_{jdlm} - z_{jdmk}) \qquad \forall\, d \in D,\, \forall\, j \in N_V,\, \forall\, m \in \{N: m \neq j\},\, \forall\, l \in \{N: l \neq m\},\, \forall\, k \in \{N: k \neq m\} \tag{25}$$

$$dst_{mkd} \leq dst_{lmd} - l_{lm} + M3 \times (2 - z_{jdlm} - z_{jdmk}) \qquad \forall\, d \in D,\, \forall\, j \in N_V,\, \forall\, m \in \{N: m \neq j\},\, \forall\, l \in \{N: l \neq m\},\, \forall\, k \in \{N: k \neq m\} \tag{26}$$

$$dst_{lmd} \leq \sum_{j \in N_v} M3 \times z_{jdlm} \qquad \forall\, d \in D,\, \forall\, l \in N,\, \forall\, m \in N \tag{27}$$

Vehicle-drone integrating constraints:

$$b_{ijd} \leq \sum_{l \in N_c} z_{jdli} \qquad \forall\, d \in D,\, \forall\, i \in N_V,\, \forall\, j \in N_V \tag{28}$$

$$b_{ijd} \geq z_{jdki} \qquad \forall\, d \in D,\, \forall\, j \in N_V,\, \forall\, k \in N_C,\, \forall\, i \in N_V \tag{29}$$

$$f_{jd} \leq \sum_{m \in N_c} z_{jdjm} \qquad \forall\, d \in D,\, \forall\, j \in N_V \tag{30}$$

$$f_{jd} \geq z_{jdjk} \qquad \forall\, d \in D,\, \forall\, j \in N_V,\, \forall\, k \in N_C \tag{31}$$

$$\sum_{\substack{k \in N_1 \\ k \neq i}} x_{dki} + \sum_{j \in N_V} \sum_{m \in N_c} z_{jdmi} = \sum_{\substack{k \in N_1 \\ k \neq i}} x_{dik} + \sum_{m \in N_c} z_{idim} \qquad \forall\, d \in D,\, \forall\, i \in N_V \tag{32}$$

$$x_{dij} \leq y_{ij} \qquad \forall\, d \in D,\, \forall\, i \in N_1,\, \forall\, j \in \{N_1: j \neq i\} \tag{33}$$

$$\sum_{k \in N_1} y_{ki} \geq b_{ijd} \qquad \forall\, d \in D,\, \forall\, i \in N_V,\, \forall\, j \in N_V \tag{34}$$

$$y_{ji} \geq y_{ij} + M1 \times (b_{ijd} - 1) \qquad \forall\, d \in D,\, \forall\, i \in N_V,\, \forall\, j \in N_V \tag{35}$$

$$\sum_{k \in N_1} d_{ki} \geq \sum_{m \in N_1} d_{mj} - M1 \times (1 - b_{ijd}) \quad \forall\, d \in D,\, \forall\, i \in N_V,\, \forall\, j \in N_V \tag{36}$$

$$\sum_{k \in N_1} x_{dki} + \sum_{\substack{j \in N_V \\ j \neq i}} b_{ijd} \geq f_{id} \quad \forall\, d \in D,\, \forall\, i \in N_V \tag{37}$$

$$b_{ijd} \leq f_{jd} \quad \forall\, d \in D,\, \forall\, i \in N_V,\, \forall\, j \in N_V \tag{38}$$

$$u_i - u_j + N_1 \times y_{ij} \leq N_1 - 1 \quad \forall\, i \in N_1,\, \forall\, j \in \{N_v\colon j \neq i\} \tag{39}$$

$$u_0 = 1 \tag{40}$$

$$y_{ij} \in \{0, 1\},\, x_{dij} \in \{0, 1\},\, z_{jdlm} \in \{0, 1\},\, b_{ijd} \in \{0, 1\},\, f_{jd} \in \{0, 1\},\, dw_{lmd} \geq 0,\, pw_{lmd} \geq 0,\, dst_{lmd} \geq 0,\, d_{ij} \geq 0,\, 1 \leq u_i$$
$$\leq Nv(size) + 2 \quad \forall\, d \in D,\, \forall\, i \in N_1,\, \forall\, j \in N_1,\, \forall\, l \in N,\, \forall\, m \in N \tag{41}$$

The objective function given in (1) minimizes the total operation cost for the multimodal network. The first term represents the operation cost of the tour constructed for the vehicle to dispatch and collect the drones. The second term represents the operation cost of the tours constructed for the drones to visit all customers. Constraints (2) and (3) ensure that the vehicle starts and ends its tour at the depot. Constraint (4) ensures that all drones return back to the depot.

Constraint (5) guarantees path continuity for the vehicle. Constraints (6)–(9) track the distance traveled by the vehicle as it moves out from the depot or any intermediate station. These constraints are nonbinding if the vehicle does not travel on link $(i, j)$. Thus, constraint (10) ensures that $d_{ij} \,\forall\, (i, j) \in A$ is equal to zero if the vehicle does not traverse link $(i, j)$.

Constraints (11)–(27) ensure the feasibility of the tours constructed for each drone. Constraints (11) and (12) state that each drone starts its tour from its dispatching station. Constraint (13) ensures that each customer is served by one drone. Constraint (14) guarantees the continuity of the tour constructed for each drone. Drones cannot be loaded beyond their maximum carrying load capacity as described in constraint (15). Constraint (16) ensures that each drone leaves the vehicle carrying the required delivery load to serve its designated customers. Constraints (17)–(20) update the delivery and pick-up carrying load for each drone at each customer node. Constraints (21) and (22) ensure that $dw_{lmd}$ and $pw_{lmd}$ are equal to zero, if drone $d \in D$ does not travel on link $(l, m) \in A$. Constraints (23)–(27) ensure that the flight range for each drone is not violated. Constraint (23) mandates that each drone starts its tour with a fully charged battery (i.e., full flight range). Constraint (24) ensures that the drone's flight range is sufficient for the drone to reach its destination. Constraints (25) and (26) update the remaining flight range based on the traveled distance for each drone. Constraint (27) ensures that the available flight range (battery lifespan) for a drone is not decremented if a link is not traveled by that drone.

The remaining constraints capture the interactions between the vehicle and drones for dispatch and collection. Constraint (28) states that the decision variable $b_{ijd}$, which defines the dispatching and collection stations for drone $d \in D$, is equal to one if the drone dispatched from station $j \in N_V$ is collected at station $i \in N_V$. Note that the same station could be used for dispatching and collecting the drone, that is $i = j$. Constraint (29) requires that if a drone returns to a station, the vehicle must pick-up that drone from that station. Constraint (30) and (31) ensure that the value of the decision variable $f_{jd}$, which is used to specify the dispatching station of the drone, is equal to one if drone $d \in D$ is dispatched from station $j \in N_V$. Constraint (32) guarantees drone flow conservation at all stations. Constraint (33) ensures that the vehicle can carry a drone a long a link only if the vehicle is scheduled to travel on that link. Constraint (34) requires that the vehicle visits the collection station where the drone is scheduled to return. Constraints (35) and (36) ensure that if a drone is dispatched and collected from two different stations, the vehicle must visit the dispatching station before the collection station. In constraint (37), the drone must be collected by the vehicle to replace/recharge its battery and load it with a new set of packages before it is dispatched. Constraint (38) states that a drone cannot be collected if it was not dispatched in the first place. Sub-tour elimination is provided by constraints (39) and (40). Finally, constraint (41) forces the binary and non-negativity conditions for the variables.

To understand the complexity of the HVDRP, one can view its formulation as an extension of the conventional formulation of the VPR (I) to construct the vehicle route, (II) to construct the drone routes, and (III) to ensure correct integration of the two modes. Thus, the complexity for the HVDRP depends on the complexity of these three problem components. For the vehicle routing decisions, in addition to determining the set of visited stations and their sequence in the tour, the problem also entails deciding on the dispatching and collection of drones at different stations and the transportation of drones by the vehicle along different links. The vehicle routing component of the HVDRP is an NP-hard problem where the number of solutions grows exponentially with the number of stations in the network. For the drone routing decisions, the problem is an extension of the CVRP, where each drone is modeled as a vehicle with limited capacity (i.e., flying range and the load carrying capacity). It requires determining feasible routes for all drones, where each drone route is defined in terms of its dispatching and collecting stations, the set of customers to be visited, and the sequence by which these customers are inserted in the drone route. The drone routing component is also NP-hard as the number of solutions grows exponentially with the number of stations and customers in the network. Thus, to appreciate the level of complexity of the HVDRP, one should try to answer the following question: do the vehicle-drone integration constraints specifically introduced to model the mothership system reduce the search space for the vehicle and drone routing decisions? Considering the interdependence between the vehicle and the drone routing decisions, their solution spaces cannot be reduced a priori. The HVDRP requires examining the combinations of the vehicle and the drone routing decisions, while ensuring the feasibility of the integrated solution with respect to

station visitation sequencing, to determine the optimal integrated vehicle-drone routing scheme. This additional check has a combinatorial complexity considering the routing combinations for the vehicle and the drones in constructing integrated solutions. As such, the HVDRP is an NP-hard problem with a higher level of complexity compared to the conventional VRP and the CPRP. Thus, obtaining provably optimal solutions using this formulation for the HVDRP are limited to small problem instances, and efficient methodologies are needed in order to provide good solutions within a practical running time to suit real-world applications of the mothership system.

## 5. Solution methodology

As mentioned earlier, the HVDRP defined above is an NP-hard problem. As such, finding the exact optimal solution in a reasonable execution time is limited only to small-size problems. In this section, we present three heuristics-based solution methodologies that are developed to find a near-optimal solution for the problem. The heuristics extend the Clarke and Wright (CW) algorithm to consider the multimodality of the integrated vehicle-drone routing problem (Clarke and Wright, 1964). The CW algorithm uses the saving matrix concept to rank the merging process of two sub-routes into one large route. For the two nodes $i$ and $j$ with distance $l_{ij}$, the saving $\vartheta_{ij}$ is calculated as follows:

$$\vartheta_{ij} = l_{i0} + l_{0j} - l_{ij} \tag{42}$$

where $l_{i0}$ and $l_{0j}$ are the distances from nodes $i$ and $j$ to the depot node 0, respectively. This concept can be applied to the HVDRP to construct the vehicle route and the drone routes. For the vehicle, nodes $i$ and $j$ represent dispatching and collection stations while node 0 represents the depot. For a drone route, nodes $i$ and $j$ represent customers. The depot(s) for the drone is the closest station to the first visited customer and the closest station to the last visited customer. For each customer $i$, the closest station $s_i$ is determined such that:

$$l_{is_i} = \min\left(l_{is_k} \; \forall \; s_k \in N_V\right) \tag{43}$$

Thus, the saving expression for a drone becomes:

$$\vartheta_{ij} = l_{is_i} + l_{s_jj} - l_{ij} \tag{44}$$

In Eq. (44), $s_i$ and $s_j$ could be the same station if it is the closest to both customers, or two different stations if the closest station to customer $i$ is different from that of customer $j$. For example, consider the network in Fig. 1, customers 16 and 17 are close to stations 4 and station 5, respectively. Thus, their saving is calculated as follows:
$\vartheta_{16-17} = l_{16-4} + l_{5-17} - l_{16-17} = 2.83 + 2.83 - 1 = 4.66$ miles
On the other hand, customers 20 and 21 are both close to station 8 resulting in the following saving:
$\vartheta_{20-21} = l_{20-8} + l_{8-21} - l_{20-21} = 1.80 + 1.41 - 0.5 = 2.71$ miles
The following subsections describe the three heuristics developed for the HVDRP, namely the HCWH, the VDH and the DDH. The three heuristics consist of two route building procedures implemented in an iterative framework, one for the vehicle and one for the



| Node | X (mile) | Y (mile) | PW (lbs.) | DW (lbs.) |
|------|------|------|------|------|
| 0 | 0.0 | 0.0 | - | - |
| 1 | 5.0 | 0.0 | - | - |
| 2 | 10.0 | 0.0 | - | - |
| 3 | 0.0 | 5.0 | - | - |
| 4 | 5.0 | 5.0 | - | - |
| 5 | 10.0 | 5.0 | - | - |
| 6 | 0.0 | 10.0 | - | - |
| 7 | 5.0 | 10.0 | - | - |
| 8 | 10.0 | 10.0 | - | - |
| 9 | 6.0 | 2.0 | 5.0 | 2.0 |
| 10 | 12.0 | 2.0 | 0.0 | 4.0 |
| 11 | 2.0 | 4.0 | 1.0 | 3.0 |
| 12 | 3.0 | 4.0 | 2.0 | 4.0 |
| 13 | 7.0 | 3.0 | 2.0 | 3.0 |
| 14 | 12.0 | 3.0 | 2.0 | 3.0 |
| 15 | 3.0 | 7.0 | 1.0 | 2.0 |
| 16 | 7.0 | 7.0 | 2.0 | 3.0 |
| 17 | 8.0 | 7.0 | 1.0 | 3.0 |
| 18 | 3.0 | 8.0 | 5.0 | 1.0 |
| 19 | 2.0 | 12.0 | 2.0 | 2.0 |
| 20 | 9.0 | 11.5 | 0.0 | 2.0 |
| 21 | 9.0 | 11.0 | 1.0 | 3.0 |

Vehicle cost = $2.0/mile
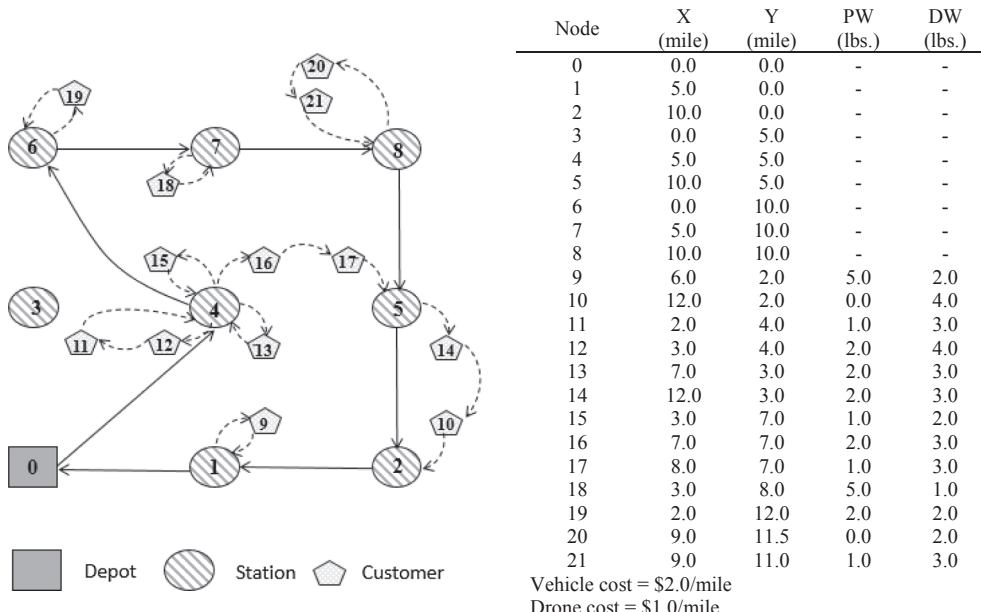Drone cost = $1.0/mile

**Fig. 1.** An example of a multimodal vehicle-drone network.

drones. For simplicity, we assume a fleet of identical drones in terms of their flight range, $r$, and load carrying capacity, $w$. The HCWH constructs vehicle route and drone routes such that the total network cost is minimized. It adopts a multimodal cost-reduction greedy strategy that combines vehicle and drone cost savings to construct efficient intermodal routes that minimize the total operation cost for the vehicle and drones. In the VDH, the vehicle route is first optimized ignoring the drone routes, resulting in a set of stations that can be used to dispatch and collect the drones. Given this set of stations, efficient drone routes are then determined. The process is iterated to eliminate stations of high cost from the vehicle route while ensuring solution feasibility. The DDH, on the other hand, first optimizes the drone routes to determine the set of dispatching and collection stations. An efficient vehicle route is then constructed to visit these stations, taking into consideration that the dispatching station is visited before the collection station for each drone. As such, both the VDH and DDH implement single-mode cost-reduction greedy strategies with respect to the vehicle and the drones, respectively, while the HCWH implements a multimodal cost-reduction strategy that simultaneously minimizes the cost of both modes. Even though the VDH and the DDH provide platforms to benchmark the performance of the HCWH, these two heuristics could be valuable for certain problems. For example, in problem instances where the vehicle's operation cost is much higher than that of the drone's cost, the solution generated by the VDH, which gives high priority to the optimization of the vehicle route, is expected to be close to the optimal solution. On the other hand, for problem instances in which the drone's operation cost is relatively high, the DDH is likely to generate near-optimal solutions, as it optimizes the routes of multiple drones over the route of one vehicle.

### 5.1. The hybrid Clarke and Wright heuristic (HCWH)

The HCWH is an iterative procedure, where each iteration includes the following five steps.

Step 1: calculate the route savings of the vehicle and the drones using Eqs. (42) and (44), respectively.
Step 2: calculate the integrated vehicle and drone (multimodal) route savings.
Step 3: using the multimodal savings, construct the most efficient vehicle route.
Step 4: using the drone savings, construct the most efficient drone routes considering the vehicle route constructed in Step 3.
Step 5: examine the elimination the station with the highest saving in the total cost.

In Step 1, the heuristic separately calculates the cost savings for the vehicle and the drones. The elements in the vehicle saving list are obtained using Eq. (42), while the elements in the drone saving list are obtained using Eq. (44). Step 2 ensures that the saving associated with merging a pair of stations in the vehicle route is calculated such that it considers the saving in the vehicle routing cost and the saving in the drone routing cost. Thus, a term to capture the drone saving is added to the vehicle saving, as given in Eq. (45).

$$\vartheta_{ij} = (l_{j0} + l_{0i} - l_{ij}) \cdot c_v + (l_{im} + l_{nj} - l_{mn}) \cdot c_d \tag{45}$$

where, nodes $m$ and $n$ are customer nodes. Stations $i$ and $j$ are the origin and the destination of the merged drone route, respectively. Furthermore, $c_v$ and $c_d$ are the vehicle's and drones' operation cost per unit distance, respectively.

To elaborate more on Eq. (45), consider the example in Fig. 2. The multimodal cost saving step loops over the drone saving elements to construct feasible drone routes. As shown in the figure, if customers $m$ and $n$ are merged in a feasible drone route that is dispatched from station $i$ and collected at a different station $j$, the saving associated with the merge of these two customers is added to the saving element of station pair $(i, j)$. In case no feasible drone route can be constructed between the two stations due to the limitation of the drone's flight range and/or its load carrying capacity, no drone saving is added to the vehicle saving for this station pair. Step 3 uses the multimodal vehicle saving list to construct the vehicle route. Given the vehicle route constructed in Step 3, Step 4 constructs the drone routes using the drone saving list. Finally, Step 5 checks if any station can be eliminated from the vehicle route to reduce the total cost of the network. The above steps are repeated until no station can be eliminated from the vehicle route.

As shown in Fig. 3, heuristic (H1) starts by determining the closest station for every customer using Eq. (43). Then, the elements of the drone cost savings list, $\psi_D$, are calculated using Eq. (44) and the resulting list is sorted in a descending order. The multimodal cost



$$Cost\ 1 = \begin{pmatrix} c_v \times (l_{i0} + l_{0i} + l_{0j} + l_{j0}) + \\ c_d \times (l_{jn} + l_{nj} + l_{mi} + l_{im}) \end{pmatrix}$$

$$Cost\ 2 = \begin{pmatrix} c_v \times (l_{i0} + l_{ij} + l_{j0}) + \\ c_d \times (l_{nj} + l_{mn} + l_{mi}) \end{pmatrix}$$

➔ $Saving = Cost\ 1 - Cost\ 2 = (l_{j0} + l_{0i} - l_{ij}) \cdot c_v + (l_{im} + l_{nj} - l_{mn}) \cdot c_d$
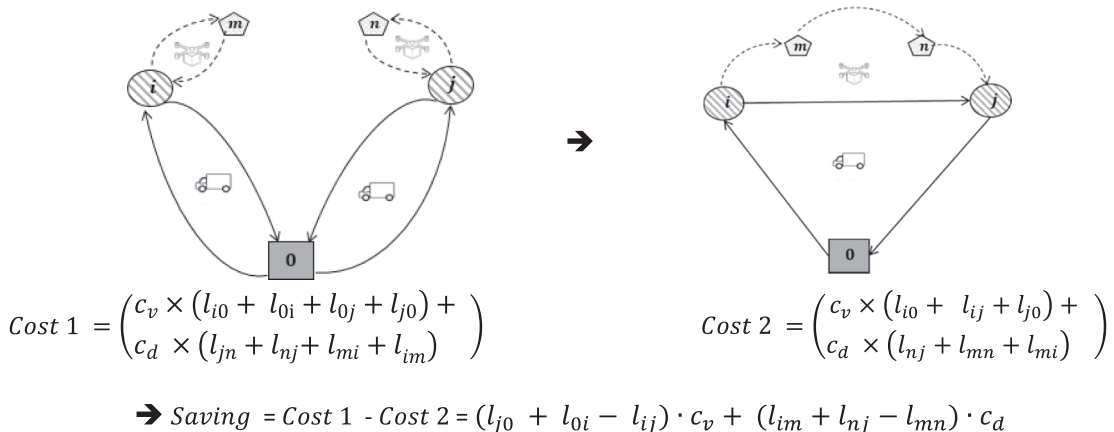
**Fig. 2.** Illustration of cost saving for the hybrid vehicle-drone routing problem.

---

**H1: The Hybrid Clarke and Wright Heuristic**

---

**Input:** Network topology and customer information

**Result:** $S_V$ and $S_D$

**repeat**

    Set the closest station for each customer considering the stations in $N_V$

    $\psi_D$ = Calculate pair saving for customers

    $\psi_V$ = Calculate_Multimodal_Saving_For_Stations($\psi_D, w, r$)

    $S_V$ = Call the CW algorithm using $N_V \cup N_D$ and $\psi_V$ as input

    $S_D$ = Build_Drone_Routes ($\psi_D, w, r$)

    Check if reversed vehicle route reduces total cost

    $stn$= Determine_Station_with_Highest_Multimodal_Saving($N_V, N_D, S_V, S_D, \psi_V, w, r$)

    **if** ($stn \neq \emptyset$) **then**

        $N_V = N_V - stn; \; S_V = \emptyset; \; S_D = \emptyset$

    **else**

        **Stop**

    **end if**

**until** (Stop)

**return** $S_V$ and $S_D$

---

**Fig. 3.** Main steps of the hybrid Clarke and Wright heuristic.

savings list, $\psi_V$, is calculated as described in heuristic (H2) and also sorted in a descending order. Next, $\psi_V$ is used as an input for the CW algorithm to construct an efficient vehicle route, $S_V$, considering all stations in the network and the depot, $N_V \cup N_D$. Assuming an identical set of drones, $\psi_D$ is used as an input for the CW algorithm to construct the drone routes given their load carrying capacity, $w$, and maximum flight range, $r$. In this step, the drones could be dispatched or collected from any station in the network. Heuristics (H3) and (H4), presented in Fig. 5 and Fig. 7 respectively, are used to construct the drone routes for a given set of dispatching and collection stations. More details on this step are given hereafter.

The heuristic then checks if reversing the vehicle route improves the total cost. In this step, the vehicle route is reversed and the corresponding drone routes are constructed. If the total cost decreases, $S_V$ and $S_D$ are updated. This step is important, as the order by which the stations are visited by the vehicle could affect the feasibility of some drone routes with respect to their load carrying capacity limitations. Next, the heuristic iteratively searches for expensive stations for possible elimination from the vehicle route. The station with the highest multimodal cost saving is determined. This station is eliminated after ensuring that all customers can be served using a feasible set of drone routes that do not start from or end at the eliminated station. An efficient vehicle route is again constructed using the CW algorithm after excluding this station. The corresponding drone routes are constructed considering the reduced set of stations. The procedure is repeated until no further stations can be eliminated from the vehicle route. A station cannot be eliminated if its elimination prevents the drones from reaching any of the customers or it results in an increase in the total routing cost.

The calculation of the multimodal cost savings is presented in Fig. 4. The heuristic starts by computing the vehicle's cost saving using Eq. (42). The savings are ranked in the descending ordered list, $\psi_V$. Next, the heuristic constructs initial drone routes, where each route includes one customer such that the drone is dispatched and collected from its nearest station. The heuristic then loops over the elements of the drone saving list, $\psi_D$. For each saving element in this list, $\vartheta_{mn}$, customers $m$ and $n$ are merged into one drone route considering the following two conditions: (a) drone's maximum flight range and its load carrying capacity are not violated, and (b) the absolute difference between the number of collected and dispatched drones at the stations does not exceed the maximum number of drones allowed on the vehicle, $MaxD$. For this drone route, if the origin station $i$ is different from the destination station $j$, then their saving element, $\vartheta_{ij}$ is modified by adding to it the saving of the merged customers, $\vartheta_{mn}$, as explained in Eq. (45). The counter of the number of drone routes between station $i$ and station $j$, $cntr_{ij}$, is incremented by one to ensure that condition (b) is satisfied. The heuristic also checks the saving for element $\vartheta_{ji}$ by reversing the drone route from customer $n$ to costumer $m$. If the reverse drone route (i.e. the origin station $i$ becomes the destination and the destination station $j$ becomes the origin) does not violate the two conditions described above, then the saving element, $\vartheta_{ji}$, is modified by adding to it the saving of the merged customers, $\vartheta_{nm}$. The counter of the number of drone routes between these stations, $cntr_{ji}$, is incremented. Finally, the elements in $\psi_V$ are sorted in a descending order to be used as an input for the construction of the vehicle route.

Heuristic (H3) presents the steps of building the drone routes as shown in Fig. 5. Building efficient drone routes is slightly more challenging than building the vehicle route. Similar to the vehicle routing step, the CW algorithm is used to build the drone routes. However, this step requires implementing two additional constraints to ensure the feasibility of merging two customers into one drone route. The first constraint ensures that the drone's maximum flight range and load carrying capacity are not violated. The second constraint ensures the feasibility of the drone routes with respect to the vehicle route. This constraint involves three operation rules. First, the absolute difference between the number of collected and dispatched drones at any station does not exceed the maximum number of drones allowed on the vehicle. Second, the drone's dispatching station must be visited by the vehicle before visiting the collection station. Finally, at every station, the vehicle must have at least one drone to serve customers around that station. To illustrate these rules, consider the network example in Fig. 6, which shows the vehicle route and the routes of two drones mounted on this vehicle. Fig. 6(a) provides a case in which the first rule is violated. At station 4, the absolute difference between the

---

**H2:** Calculate_Multimodal_Saving_For_Stations

**Input:** $\psi_D, w, r$

**Result:** $\psi_V$

$\psi_V$ = Calculate pair saving for stations

$S_D$ = Construct initial drone routes

$cntr_{ij} = 0 \; \forall \, i \in N_V, \forall \, j \in N_V$

**while** $\psi_D \neq \emptyset$ **do**

    Starting from the first element, $\vartheta_{mn}$, of $\psi_D$

    Get *route1* that contains customer $m$, and *route2* that contains customer $n$ from $S_D$

    **if** (*route1* $\neq$ *route2* & customers $m$ and $n$ are not intermediate nodes) **then**

        *merged_drone_route* = Merge customers $m$ and $n$ in new route with origin $i$ and destination $j$

        **if** $(\sum_k (pw_k + dw_k) \leq w \; \& \; \sum_{\acute{m}\acute{n}} l_{\acute{m}\acute{n}} \leq r \; \& \; cntr_{ij} \leq MaxD)$ **then**

            Remove *route1* and *route2* from $S_D$ and add *merged_drone_route* to $S_D$

            **if** $(i \neq j)$ **then**

                $cntr_{ij} = cntr_{ij} + 1; \; \vartheta_{ij} = \vartheta_{ij} \cdot c_v + \vartheta_{mn} \cdot c_d$; overwrite $\vartheta_{ij}$ in $\psi_V$

                *reversed_merged_drone_route* = Reverse *merged_drone_route*

                **if** $(\sum_k (pw_{\acute{k}} + dw_{\acute{k}}) \leq w \; \& \; \sum_{\acute{n}\acute{m}} l_{\acute{n}\acute{m}} \leq r \; \& \; cntr_{ji} \leq MaxD)$ **then**

                    $cntr_{ji} = cntr_{ji} + 1; \; \vartheta_{ji} = \vartheta_{ji} \cdot c_v + \vartheta_{nm} \cdot c_d$; overwrite $\vartheta_{ji}$ in $\psi_V$

                **end if**

            **end if**

        **end if**

    **end if**

    Eliminate $\vartheta_{mn}$ from $\psi_D$

**End**

Sort $\psi_V$ in descending order

**return** $\psi_V$

---

Fig. 4. Procedure for calculating multimodal cost savings for stations.

---

**H3:** Build_Drone_Routes

**Input:** $\psi_D, w, r$

**Result:** $S_D$

$S_D$ = Construct initial drone routes

**while** $\psi_D \neq \emptyset$ **do**

    Starting from the first element, $\vartheta_{ij}$, of $\psi_D$

    Get *route1* that contains customer $i$, and *route2* that contains customer $j$ from $S_D$

    **if** (*route1* $\neq$ *route2* & customers $i$ and $j$ are not intermediate nodes) **then**

        *merged_route* = Merge customers $i$ and $j$ in a new route

        **if** $(\sum_k (pw_k + dw_k) \leq w \; \& \; \sum_{mn} l_{mn} \leq r \; \&$

        *merged_route* is feasible from the vehicle's perspective) **then**

            **if** (the nearest station of any customer in *merged_route* is neither $O$ nor $D$) **then**

                *merged_route* = Improve_Drone_Route(*merged_route*)

            **end if**

            Remove *route1* and *route2* from $S_D$

            Add *merged_route* to $S_D$

        **end if**

    **end if**

    Eliminate $\vartheta_{ij}$ from $\psi_D$

**End**

**return** $S_D$

---

Fig. 5. Procedure for building the drone routes.

number of collected and dispatched drones is four, which is greater than the number of drones carried by the vehicle. Fig. 6(b) shows a case that violates the second rule. Because the vehicle visits station 2 before station 5, the drone route that starts at station 5 and ends at station 2 is infeasible. Fig. 6(c) gives an example of the violation of the third rule, since the vehicle arrives at station 8 with no drones onboard, which makes it infeasible to serve customers at nodes 20 and 21.

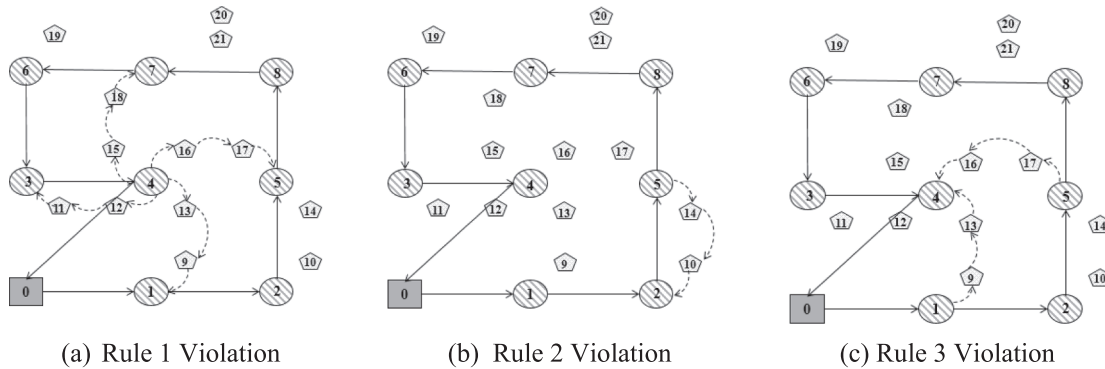(a) Rule 1 Violation     (b) Rule 2 Violation     (c) Rule 3 Violation

Fig. 6. An example of a multimodal vehicle-drone network with operation violations.

After completing the step of merging two customers in a drone route, the heuristic checks if the drone route could be further improved by re-ordering the customers along the route. As shown in Fig. 7, the heuristic (H4) checks if the nearest station to any of the customers in set $N'_C$ served in that route, as determined in Eq. (43), is neither the origin, $O$, nor the destination, $D$, of the route. If a customer has another station as its nearest station, the nearest station of that customer is over-written to be the closest of the origin or the destination of the route. The cost saving matrix, $\psi_{New}$, for the customers served in the route is recalculated after over-writing their nearest station. Then, the route is rebuilt based on the new saving matrix resulting in a more efficient sequence of customer nodes. The new route is checked against the drone's flight range and load carrying capacity limits. If the constraint is satisfied, the algorithm returns the modified route. Otherwise, it maintains the original route as the most efficient route.

As mentioned above, at each iteration, a search procedure is implemented to determine the station along the vehicle route with the highest cost saving. Following the steps of heuristic (H5) presented in Fig. 8, the procedure applies a simple linear search to determine the station, $stn$, with the highest cost saving, $\vartheta_{stn}$. The cost calculation in this step requires calculating the vehicle routing cost savings and the drone extra cost associated with removing this station. A feasibility check is implemented to ensure that customers close to a potentially eliminated station are reachable by a drone from any of the remaining stations, $N'_V$, in the vehicle route. For example, consider the network presented in Fig. 1, assuming the drone's maximum flight range is 7.0 miles, removing station 6 is infeasible as customer 19 cannot be served from station 7. A round trip of 7.2 miles to reach customer 19 from station 7 violates the drone's maximum flight range. However, removing station 1 is feasible as customers 9 can still be served from station 4. The length of the round trip to serve customer 9 from station 4 is 6.3 miles.

## 5.2. The vehicle-driven heuristic (VDH)

The steps of the VDH are similar to the ones described in Fig. 3, with the exception of the method used to calculate the cost savings for routing the vehicle. Here, the cost savings for the vehicle do not consider the drone cost savings. Thus, the VDH gives priority to reducing the routing cost of the vehicle over that of the drones. Similar to the HCWH, the heuristic starts by generating an initial vehicle route in which the vehicle visits all stations in the network. In this step, the CW algorithm is used to generate an efficient route for the vehicle using the vehicle cost saving matrix calculated using Eq. (42). Drone routes are then constructed assuming that the drones can be dispatched and collected from any station in the network. Here, the drone savings are calculated using Eq. (44). One should note that this heuristic does not include the step of checking if reversing the vehicle route will reduce the total cost as it

---

**H4: Improve_Drone_Route**

**Input:** *route*
**Result:** *improved_route*
**for all** $(j \in N'_c)$ **do**
  **if** $(s_j$ is neither $O$ nor $D)$ **then**
$$s_j = \begin{cases} O \ if \ (l_{oj} \leq l_{Dj}) \\ D \quad otherwise \end{cases}$$
  **end if**
**end for**
Recalculate $\psi_{New}$ based on the new closest station for customers in $N'_c$
*improved_route* = Rebuild the route based on the new saving matrix $\psi_{New}$
**if** $(\sum_k (pw_k + dw_k) \leq w \ \& \ \sum_{mn} l_{mn} \leq r)$ **then**
  **return** *improved_route*
**end if**
**return** *route*

Fig. 7. Procedure for improving the drone route.

---

**H5:** Determine_Station_with_Highest_Multimodal_Saving

---

**Input:** $N_V, N_D, S_V, S_D, \psi_V, w, r$

**Result:** $stn$

$N'_V = N_V$

**for all** $(j \in N_V)$ **do**

    Remove Station $j$ from $N'_V$

    **if** (customers close to station $j$ are reachable by the drone from any station in $N'_V$) **then**

        Set the closest station for each customer considering the stations in $N'_V$

        $\psi'_D$ = Calculate pair saving for customers

        $S'_V$ = Call the CW algorithm using $N'_V \cup N_D$ and $\psi_V$ as input

        $S'_D$ = Build_Drone_Routes $(\psi'_D, w, r)$

        $\vartheta_j$ = cost $(S_V)$ − cost $(S'_V)$ + cost $(S_D)$ − cost $(S'_D)$

        **if** $(\vartheta_j > 0)$ **then**

            Add the saving element $\vartheta_j$ to $\psi$

        **end if**

        $S'_V = \varnothing; S'_D = \varnothing; \psi'_D = \varnothing$

    **end if**

    $N'_V = N_V$

**end for**

Sort the element in $\psi$ in a descending order

$stn$ = station corresponding to the first element, $\vartheta_{stn}$, in the sorted list $\psi$

**return** $stn$

---

Fig. 8. Procedure for determining the station with the highest cost along the vehicle route.

focuses on reducing the vehicle routing cost. Next, as the heuristic adopts a greedy strategy with respect to the vehicle routing cost, it iteratively searches for stations which are expensive for the vehicle to visit while ignoring any extra drone routing cost associated with removing this station. The station with the highest vehicle cost saving is eliminated after ensuring that all customers can be visited from the remaining stations. The vehicle route and the drone routes are reconstructed considering the reduced set of stations. The process is iterated until no other stations can be eliminated from the vehicle route.

## 5.3. The drone-driven heuristic

Unlike the VDH, the DDH gives priority to reducing the routing cost of the drones over the vehicle. Hence, it constructs the drone routes before the vehicle route. The main steps of the DDH are presented in Fig. 9. The heuristic (H6) incrementally constructs drone routes while ensuring that the resulting set of drone dispatching and collection stations can be served by one vehicle. The CW

---

**H6: The Drone-Driven Heuristic**

---

**Input:** Network topology and customers information

**Result:** $S_V$ and $S_D$

Set the closest station for each customer considering the stations in $N_V$

$\psi_D$ = Calculate pair saving for customers

$\psi_V$ = Calculate pair saving for stations

$S_D$ = Build_Drone_Routes $(\psi_D, w, r)$

$S_V$ = Construct initial vehicle routes

**while** $\psi_V \neq \varnothing$ **do**

    Starting from the first element, $\vartheta_{ij}$, of $\psi_V$

    Get *route1* that contains station $i$, and *route2* that contains station $j$ from $S_V$

    **if** (*route1* $\neq$ *route2* & stations $i$ and $j$ are not intermediate nodes) **then**

        *merged_vehicle_route* = Merge station $i$ and station $j$ in a new route

        **if** (*merged_vehicle_route* is feasible from the drones' perspective) **then**

            Remove *route1* and *route2* from $S_V$

            Add *merged_vehicle_route* to $S_V$

        **end if**

    **end if**

    Eliminate $\vartheta_{ij}$ from $\psi_V$

**End**

**return** $S_V$ and $S_D$

---

Fig. 9. Main steps of the drone-driven heuristic.

HCWH Solution

VDH Solution

DDH Solution



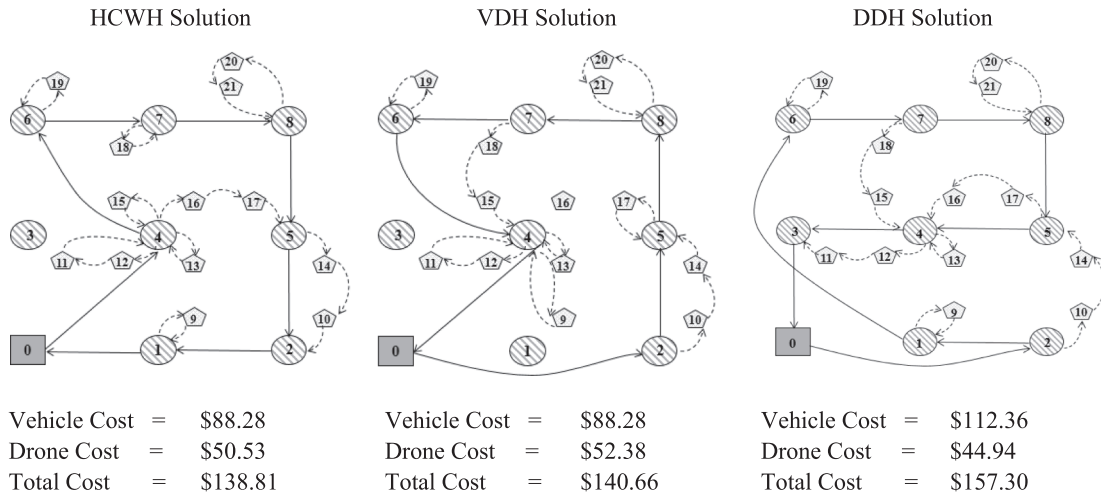| | HCWH | | VDH | | DDH |
|---|---|---|---|---|---|
| Vehicle Cost | = $88.28 | Vehicle Cost | = $88.28 | Vehicle Cost | = $112.36 |
| Drone Cost | = $50.53 | Drone Cost | = $52.38 | Drone Cost | = $44.94 |
| Total Cost | = $138.81 | Total Cost | = $140.66 | Total Cost | = $157.30 |

**Fig. 10.** Example to demonstrate the performance of the HCWH, VDH and DDH.

algorithm using the drone cost saving matrix calculated with Eq. (44) is used to construct the drone routes. The newly generated drone route is added to the existing set of drone routes resulting in an updated set of drone dispatching and collection stations. The CW algorithm is then activated to generate an efficient vehicle route. If the vehicle routing problem becomes infeasible, this new drone route is ignored and the next most efficient drone route is generated instead. The process continues until all customers are served and a feasible vehicle route is constructed to dispatch and collect all drones.

Similar to the HCWH, building a feasible drone route requires satisfying the three operation rules described in Fig. 6. However, in the DDH, only the first rule is considered as part of the drone route building procedure. The other two rules are moved to the vehicle route building procedure. In other words, the first rule, which ensures that the absolute difference between the number of drones dispatched and number of drones collected at any station is less than the maximum number of drones mounted on the vehicle, is mandated while constructing the drone routes. The second and the third rules are enforced while building the vehicle route, which require visiting the dispatching stations before the collection stations and ensuring that at any station there is at least one drone to serve nearby customers.

The problem given in Fig. 1 is solved using these three heuristics. The obtained solutions are presented in Fig. 10, which illustrates the difference in the solutions as they adopt different strategies for routing cost optimization. The HCWH provides the solution with the least total routing cost. A total cost of $138.81 is recorded for the HCWH solution compared to $140.66 and $157.30 for the VDH solution and the DDH solution, respectively. As the VDH adopts a vehicle-based cost reduction strategy, it gives a solution in which station 1 is eliminated from the vehicle route. The HCWH solution kept this station as part of the vehicle route, as its elimination causes an increase in the multimodal cost. Finally, while the DDH significantly reduces the drone routing cost, the corresponding vehicle routing cost is the highest among all three heuristics, causing the total cost to be the highest.

## 6. Results and analysis

In this section, we present the results of a set of experiments that are conducted to examine the performance of the three heuristics described above. To avoid bias related to the data generation, we used a common grid network with randomly generated demand in terms of location and pick-up/delivery loads. We considered networks with different numbers of stations, numbers of customers, and density levels. To avoid solution infeasibility, we made sure that (a) the distance between any two stations was less than the drone's minimum flight range, and (b) the pick-up/delivery load of any customer was less than the drone's load carrying capacity.

Seven roadway networks of a grid structure covering service areas that range from 25.0 to 500.0 square miles are considered. Stations for drone dispatching and collection are assumed to be located at the intersection nodes in these networks. These intersection nodes are spaced at a 5.0 mile distance. Customers are randomly distributed in the area with densities that range from 0.1 customer per square mile to 1.0 customer per square mile. The number of customers ranges from six customers in the smallest network to 100 customers in the largest network. Each customer is associated with a pick-up weight and/or a delivery weight that are randomly generated following the uniform distribution $U$ (0.0lbs, 5.0lbs). One vehicle equipped with two drones is used to serve these customers, unless specified otherwise. The vehicle operation cost is assumed to be twice that of the drones. The vehicle depot was assumed to be located at the southwest corner of the grid networks. Both drones are assumed to have a maximum flight range of 7.0 miles and a load carrying capacity of 10.0 lbs. Such values are in the range of the drone specifications used by UPS in their drone delivery field experiment (McFarland, 2017). Table 1 summarizes the configuration of these seven networks. For each network, 10 random instances are generated representing different spatial distributions of the customers. All runs were carried out on a Dell workstation with 72 logical processors of 3.1 GHz and 192 GB memory.

**Table 1**

Summary of network configurations used to test the performance of the heuristics.

| Network | Number of customers | Number of stations | Area (mile$^2$) | Customer density (customer/mile$^2$) |
|---------|--------------------|--------------------|-----------------|--------------------------------------|
| A1 to A5 | 6 | 3 | 25 | 0.24 |
| A6 to A10 | 8 | 3 | 25 | 0.32 |
| B1 to B10 | 50 | 8 | 100 | 0.50 |
| C1 to C10 | 50 | 15 | 300 | 0.17 |
| D1 to D10 | 50 | 24 | 500 | 0.10 |
| E1 to E10 | 100 | 8 | 100 | 1.00 |
| F1 to F10 | 100 | 15 | 300 | 0.30 |
| G1 to G10 | 100 | 24 | 500 | 0.20 |

### 6.1. Comparison with the exact optimal solution

The performance of the HCWH, VDH and DDH, which are implemented in Java version 8.0, are compared against the exact solution obtained by CPLEX 12.6.1 Java callable libraries (IBM, 2009), which is used to solve the MIP presented in Section 4. The total routing cost and the execution time are reported for all tested cases. Considering the large execution time required to obtain the exact solution using CPLEX, these results are reported only to the small networks A-1 to A-10 as their solutions can be obtained within a reasonable timeframe (less than six hours). Table 2 gives a summary of the performance comparison results. As shown in the table, the three heuristics produce the exact optimal solution for most tested networks. While the HCWH generates the exact solutions for all networks, the VDH and DDH generate the exact solutions for nine and six networks out of the ten tested networks, respectively. In addition, for cases in which the optimal solution is not obtained, the optimality gaps recorded for the VDH are generally lower than those of the DDH.

The three heuristics significantly outperform CPLEX in terms of the execution time. For example, for network A-1, the exact optimal solution using CPLEX is obtained in about 11.7 s. The execution times for the three heuristics are less than 0.02 s for that network. One can also observe the large increase in the execution time using CPLEX when the number of customers is increased from six customers (networks A-1 to A-5) to eight (networks A-6 to A-10). For example, the execution time jumped to 17,056.5 s for A-6 compared to 11.7 s for A-1. Such substantial increase in the execution time with the increase in the number of customers is not observed for any of the three heuristics. The highest execution time for A-6 to A-10 networks is less than 0.10 s.

The results in Table 2 show that the HCWH was able to find the optimal solution for all studied instances. Additionally, a randomly generated problem instance of 8 customers and 5 stations is considered. For this problem instance, we used the solution obtained from the HCWH as a warm start (initial solution) for CPLEX. While CPLEX's optimal solution was not obtained within an execution time of up to 24 h, CPLEX was able to find four incumbent solutions that are better than the one obtained by the HCWH with an improvement in the objective function of 7.35%. The results of this test illustrates that there could be cases in which CPLEX produces solutions with better performance than those obtained by the HCWH.

### 6.2. Performance comparison for large network instances

The performance of the three heuristics is again compared considering large problem instances. Six different networks are used in this comparison which includes 50 customers (networks B, C and D) and 100 customers (networks E, F and G), respectively. As given in Table 3 and Table 4, each network is tested for 10 random instances. For each instance, the routing cost is reported for the vehicle ($C_V$), the drones ($C_D$), and the entire network ($C_{Total}$). The number of stops made by the vehicle to dispatch and collect the drones, η, and the total number of drone dispatches, ή, to serve the customers also are given. Finally, the execution time for each problem instance is recorded. The average of the 10 random instances is given for each network. As shown in the tables, the solution obtained using the HCWH provides the best cost performance for the majority of the tested problem instances. The VDH outperformed the

**Table 2**

The heuristics' performance comparison with the optimal solution.

| Instance | Exact solution (CPLEX) | | HCWH | | | VDH | | | DDH | | |
|----------|-----------|--------------|-----------|--------------|---------|-----------|--------------|---------|-----------|--------------|---------|
| | Cost ($) | Runtime (sec) | Cost ($) | Runtime (sec) | Gap (%) | Cost ($) | Runtime (sec) | Gap (%) | Cost ($) | Runtime (sec) | Gap (%) |
| A-1 | 46.8 | 11.710 | 46.8 | 0.019 | 0 | 46.8 | 0.016 | 0 | 46.8 | 0.016 | 0 |
| A-2 | 50.3 | 99.674 | 50.3 | 0.017 | 0 | 50.3 | 0.015 | 0 | 50.3 | 0.016 | 0 |
| A-3 | 50.6 | 12.095 | 50.6 | 0.035 | 0 | 50.6 | 0.026 | 0 | 55.7 | 0.016 | 9.0 |
| A-4 | 46.2 | 59.108 | 46.2 | 0.038 | 0 | 46.2 | 0.026 | 0 | 60.1 | 0.037 | 23.0 |
| A-5 | 50.0 | 62.296 | 50.0 | 0.032 | 0 | 50.0 | 0.024 | 0 | 50.8 | 0.037 | 1.0 |
| A-6 | 60.5 | 17056.499 | 60.5 | 0.031 | 0 | 60.5 | 0.016 | 0 | 60.5 | 0.031 | 0 |
| A-7 | 50.5 | 1817.953 | 50.5 | 0.032 | 0 | 50.5 | 0.020 | 0 | 50.5 | 0.031 | 0 |
| A-8 | 55.2 | 4903.824 | 55.2 | 0.032 | 0 | 56.1 | 0.031 | 2.0 | 55.2 | 0.016 | 0 |
| A-9 | 53.2 | 2722.409 | 53.2 | 0.062 | 0 | 53.2 | 0.031 | 0 | 53.2 | 0.031 | 0 |
| A-10 | 56.5 | 2113.717 | 56.5 | 0.059 | 0 | 56.5 | 0.031 | 0 | 61.2 | 0.018 | 8.0 |

**Table 3**
Performance of the heuristics for 50 customer instances.

| Instance | HCWH | | | | | | VDH | | | | | | DDH | | | | | |
|---|---|---|---|---|---|---|---|---|---|---|---|---|---|---|---|---|---|---|
| | $C_{Total}$ | $C_V$ | $C_D$ | η | ή | T | $C_{Total}$ | $C_V$ | $C_D$ | η | ή | T | $C_{Total}$ | $C_V$ | $C_D$ | η | ή | T |
| B-1 | 190.7 | 80.0 | 110.7 | 7 | 20 | 4.440 | 190.7 | 80.0 | 110.7 | 7 | 20 | 1.517 | 222.6 | 114.1 | 108.5 | 8 | 20 | 1.666 |
| B-2 | 206.5 | 94.1 | 112.4 | 8 | 21 | 1.990 | 206.5 | 94.1 | 112.4 | 8 | 21 | 0.823 | 233.1 | 120.0 | 113.1 | 8 | 22 | 1.572 |
| B-3 | 225.1 | 94.1 | 131.0 | 8 | 23 | 1.936 | 225.1 | 94.1 | 131.0 | 8 | 25 | 0.861 | 242.7 | 112.4 | 130.3 | 8 | 24 | 1.220 |
| B-4 | 221.3 | 94.1 | 127.3 | 8 | 23 | 1.840 | 219.8 | 94.1 | 125.7 | 8 | 22 | 0.827 | 249.5 | 120.0 | 129.5 | 8 | 25 | 1.847 |
| B-5 | 199.8 | 94.1 | 105.6 | 8 | 22 | 1.693 | 201.3 | 94.1 | 107.2 | 8 | 22 | 0.736 | 216.1 | 108.3 | 107.8 | 8 | 23 | 1.335 |
| B-6 | 194.3 | 94.1 | 100.2 | 8 | 19 | 1.687 | 195.2 | 94.1 | 101.1 | 8 | 19 | 0.783 | 215.6 | 114.1 | 101.5 | 8 | 20 | 1.188 |
| B-7 | 221.0 | 94.1 | 126.9 | 8 | 23 | 1.712 | 221.0 | 94.1 | 126.9 | 8 | 23 | 0.752 | 235.9 | 108.3 | 127.6 | 8 | 23 | 1.145 |
| B-8 | 193.9 | 94.1 | 99.8 | 8 | 20 | 1.721 | 196.9 | 94.1 | 102.8 | 8 | 19 | 0.739 | 224.8 | 126.5 | 98.3 | 8 | 18 | 1.156 |
| B-9 | 207.5 | 94.1 | 113.4 | 8 | 20 | 1.834 | 210.1 | 94.1 | 116.0 | 8 | 20 | 0.781 | 206.9 | 94.1 | 112.8 | 8 | 20 | 1.229 |
| B-10 | 198.1 | 94.1 | 104.0 | 8 | 21 | 1.824 | 198.1 | 94.1 | 104.0 | 8 | 21 | 0.750 | 228.1 | 120.6 | 107.5 | 8 | 21 | 1.498 |
| B mean | 205.8 | 92.7 | 113.1 | 8 | 21 | 2.068 | 206.5 | 92.7 | 113.8 | 8 | 21 | 0.857 | 227.5 | 113.8 | 113.7 | 8 | 22 | 1.386 |
| C-1 | 254.0 | 136.6 | 117.4 | 11 | 22 | 11.806 | 254.0 | 136.6 | 117.4 | 11 | 22 | 3.421 | 305.0 | 198.1 | 106.8 | 14 | 21 | 3.005 |
| C-2 | 273.2 | 148.3 | 124.9 | 13 | 28 | 6.649 | 284.9 | 148.3 | 136.6 | 12 | 27 | 2.999 | 289.9 | 166.5 | 123.4 | 14 | 25 | 2.261 |
| C-3 | 280.7 | 160.0 | 120.7 | 15 | 26 | 3.936 | 280.9 | 148.3 | 132.6 | 13 | 25 | 3.072 | 314.7 | 194.8 | 119.9 | 15 | 23 | 1.999 |
| C-4 | 264.1 | 154.1 | 110.0 | 14 | 27 | 3.611 | 266.2 | 142.4 | 123.8 | 12 | 23 | 3.211 | 276.5 | 166.5 | 110.0 | 14 | 20 | 2.349 |
| C-5 | 269.2 | 140.6 | 128.6 | 11 | 23 | 16.294 | 268.2 | 142.4 | 125.8 | 11 | 23 | 4.867 | 340.6 | 218.9 | 121.7 | 15 | 25 | 2.867 |
| C-6 | 256.6 | 128.3 | 128.3 | 11 | 24 | 8.475 | 261.7 | 128.3 | 133.4 | 11 | 25 | 2.718 | 356.7 | 234.5 | 122.2 | 13 | 22 | 2.267 |
| C-7 | 278.4 | 154.1 | 124.3 | 14 | 25 | 6.620 | 286.0 | 150.7 | 135.3 | 12 | 27 | 3.766 | 320.3 | 200.7 | 119.6 | 15 | 23 | 3.738 |
| C-8 | 275.5 | 154.2 | 121.4 | 13 | 23 | 8.060 | 286.9 | 154.2 | 132.7 | 12 | 25 | 4.016 | 329.2 | 210.5 | 118.7 | 15 | 23 | 3.348 |
| C-9 | 260.5 | 142.4 | 118.1 | 12 | 22 | 10.216 | 255.2 | 128.3 | 126.9 | 11 | 22 | 3.769 | 311.7 | 197.2 | 114.5 | 14 | 22 | 2.530 |
| C-10 | 256.1 | 128.3 | 127.8 | 11 | 24 | 8.400 | 262.5 | 136.6 | 125.9 | 11 | 24 | 2.735 | 277.8 | 160.7 | 117.1 | 13 | 23 | 1.199 |
| C mean | 266.8 | 144.7 | 122.1 | 13 | 24 | 8.406 | 270.7 | 141.6 | 129.1 | 11 | 24 | 3.457 | 312.2 | 194.8 | 117.4 | 14 | 23 | 2.556 |
| D-1 | 326.4 | 202.4 | 124.0 | 18 | 25 | 16.182 | 335.8 | 208.3 | 127.5 | 17 | 26 | 7.649 | 383.5 | 263.1 | 120.2 | 20 | 26 | 3.812 |
| D-2 | 355.7 | 216.5 | 139.2 | 18 | 28 | 30.226 | 361.7 | 216.6 | 145.1 | 17 | 30 | 11.993 | 415.3 | 279.5 | 135.8 | 22 | 29 | 3.401 |
| D-3 | 347.9 | 202.4 | 145.5 | 18 | 28 | 33.708 | 348.8 | 202.4 | 146.4 | 17 | 29 | 11.935 | 414.9 | 277.2 | 137.7 | 22 | 29 | 2.799 |
| D-4 | 376.1 | 222.4 | 153.7 | 19 | 30 | 25.122 | 356.5 | 196.5 | 160.0 | 17 | 31 | 12.840 | 442.2 | 293.1 | 149.1 | 22 | 30 | 5.601 |
| D-5 | 336.6 | 202.4 | 134.2 | 17 | 25 | 15.615 | 345.3 | 202.4 | 142.9 | 14 | 27 | 9.352 | 372.0 | 240.6 | 131.4 | 19 | 27 | 3.948 |
| D-6 | 320.1 | 193.0 | 127.1 | 15 | 25 | 22.202 | 313.6 | 186.5 | 127.1 | 15 | 25 | 8.273 | 369.3 | 250.7 | 118.6 | 19 | 24 | 2.266 |
| D-7 | 363.0 | 208.9 | 154.1 | 17 | 29 | 33.180 | 363.9 | 208.9 | 155.0 | 15 | 28 | 10.824 | 394.2 | 254.8 | 139.4 | 20 | 27 | 3.047 |
| D-8 | 356.2 | 222.4 | 133.8 | 20 | 26 | 12.937 | 347.7 | 206.5 | 141.2 | 17 | 28 | 9.051 | 397.9 | 269.0 | 128.9 | 21 | 27 | 3.461 |
| D-9 | 334.0 | 194.8 | 139.2 | 16 | 26 | 15.640 | 348.7 | 199.0 | 149.7 | 14 | 28 | 8.145 | 386.1 | 254.0 | 132.1 | 18 | 26 | 5.284 |
| D-10 | 347.4 | 222.4 | 125.0 | 19 | 25 | 12.463 | 348.5 | 222.4 | 126.1 | 19 | 26 | 7.248 | 374.1 | 254.8 | 119.3 | 21 | 25 | 3.377 |
| D mean | 346.3 | 208.8 | 137.6 | 18 | 27 | 21.728 | 347.1 | 205.0 | 142.1 | 16 | 28 | 9.731 | 394.9 | 263.7 | 131.2 | 20 | 27 | 3.699 |

$C_{Total}$: Total cost $C_V$: Vehicle cost $C_D$: Drone cost η: Number of vehicle stops ή: Number of drone dispatches T: Execution time.

HCWH in a few problem instances, as the CW algorithm does not always guarantee optimality, especially when the routed drones are constrained by a limited flight range and load carrying capacity. While the total cost obtained by the VDH and the DDH for almost all problem instances is higher than that obtained using the HCWH, the VDH and DDH provide the lowest vehicle and drone costs, respectively. These results are expected, since the VDH adopts a vehicle cost-reduction strategy and the DDH adopts a drone cost-reduction strategy. For example, the average total cost recorded for the D network using the HCWH is $346.30 with a vehicle cost of $208.80 and a drone cost of $137.60. For the VDH, the total cost increased to $347.10, while the vehicle cost was reduced to $205.00. For the DDH, the total cost increased to $394.90, while the drone cost was reduced to $131.20. A stochastic version of the HCWH is implemented to consider randomization of the saving lists. The results of this version are given in Appendix A. While the results show that there is a slight improvement in the solution quality, this improvement is associated with a significant increase in the execution time.

The three heuristics generally show comparable results in terms of the number of stops made by the vehicle and the number of drone dispatches. However, a closer look at some problem instances reveals that the VDH tends to reduce the number of stops made by the vehicle, while the DDH tends to reduce the number of drone dispatches. However, the number of stops recorded by VDH is associated with an increase in the number of drone dispatches. Similarly, the number of drone dispatches recorded by the DDH is associated with an increase in the number of vehicle stops made by the vehicle. The result is consistent with the cost-reduction strategies adopted for the two heuristics. It also resembles the split of the vehicle cost and the drone cost recorded for the solutions obtained by the VDH and the DDH, respectively. As the VDH aims at reducing the vehicle cost, it eliminates expensive stops for the vehicle at the expense of scheduling more drone dispatches. Similarly, the DDH cuts the drone cost by reducing the number of drone dispatches at the expense of more vehicle stops. For example, for network G, the VDH solution results in 21 vehicle stops and 48 drone dispatches. For the DDH solution, the number of drone dispatches decreased to 45 while the number of vehicle stops increased to 23. The HCWH produced a balanced solution in terms of number of stops made by the vehicles and the number of drone dispatches, which are recorded to be 22 and 46, respectively.

Two observations can be made regarding the heuristics' execution times. First, the execution time generally increases as the problem size increases. For example, for network B, which includes 50 customers and 8 stations, average execution times of 2.068, 0.857, and 1.386 s were recorded for the HCWH, VDH, and DDH, respectively. For network G, which includes 100 customers and 24

**Table 4**
Performance of the heuristics for 100 customer instances.

| Instance | HCWH | | | | | | VDH | | | | | | DDH | | | | | |
|---|---|---|---|---|---|---|---|---|---|---|---|---|---|---|---|---|---|---|
| | $C_{Total}$ | $C_V$ | $C_D$ | $\eta$ | $\acute{\eta}$ | T | $C_{Total}$ | $C_V$ | $C_D$ | $\eta$ | $\acute{\eta}$ | T | $C_{Total}$ | $C_V$ | $C_D$ | $\eta$ | $\acute{\eta}$ | T |
| E-1 | 257.7 | 94.1 | 163.6 | 8 | 33 | 12.512 | 257.7 | 94.1 | 163.6 | 8 | 33 | 4.132 | 288.7 | 124.7 | 164.0 | 8 | 33 | 6.762 |
| E-2 | 278.5 | 94.1 | 184.4 | 8 | 35 | 13.721 | 278.6 | 94.1 | 184.5 | 8 | 35 | 4.848 | 284.1 | 100.0 | 184.1 | 8 | 37 | 9.567 |
| E-3 | 266.0 | 94.1 | 171.9 | 8 | 37 | 13.470 | 269.7 | 94.1 | 175.6 | 8 | 35 | 4.754 | 298.9 | 126.5 | 172.3 | 8 | 36 | 9.650 |
| E-4 | 276.3 | 100.0 | 176.3 | 8 | 35 | 12.622 | 272.9 | 94.1 | 178.8 | 8 | 35 | 4.317 | 285.8 | 106.5 | 179.3 | 8 | 35 | 10.768 |
| E-5 | 259.4 | 94.1 | 165.3 | 8 | 37 | 12.530 | 260.7 | 94.1 | 166.6 | 8 | 38 | 4.348 | 286.9 | 120.7 | 166.2 | 8 | 37 | 7.974 |
| E-6 | 254.9 | 94.1 | 160.8 | 8 | 34 | 13.294 | 254.9 | 94.1 | 160.8 | 8 | 34 | 4.960 | 281.9 | 120.0 | 161.9 | 8 | 34 | 6.800 |
| E-7 | 277.6 | 94.1 | 183.5 | 8 | 39 | 15.332 | 277.6 | 94.1 | 183.5 | 8 | 39 | 5.272 | 307.0 | 126.5 | 180.5 | 8 | 39 | 10.259 |
| E-8 | 271.3 | 94.1 | 177.2 | 8 | 34 | 12.445 | 272.3 | 94.1 | 178.2 | 8 | 34 | 4.770 | 306.3 | 128.3 | 178.0 | 8 | 34 | 6.585 |
| E-9 | 288.1 | 94.1 | 194.0 | 8 | 37 | 14.381 | 289.6 | 94.1 | 195.5 | 8 | 38 | 5.224 | 310.6 | 112.4 | 198.2 | 8 | 38 | 12.629 |
| E-10 | 262.7 | 94.1 | 168.6 | 8 | 36 | 12.573 | 257.2 | 94.1 | 163.1 | 8 | 35 | 4.427 | 299.1 | 132.4 | 166.7 | 8 | 33 | 12.478 |
| E mean | 269.2 | 94.7 | 174.5 | 8 | 36 | 13.288 | 269.1 | 94.1 | 175.0 | 8 | 36 | 4.705 | 294.9 | 119.8 | 175.1 | 8 | 36 | 9.347 |
| F-1 | 384.4 | 160.0 | 224.4 | 15 | 43 | 20.967 | 381.5 | 154.1 | 227.4 | 14 | 41 | 10.526 | 407.7 | 188.3 | 219.5 | 15 | 41 | 21.384 |
| F-2 | 372.2 | 160.0 | 212.2 | 15 | 42 | 13.461 | 366.0 | 160.0 | 205.9 | 15 | 40 | 5.396 | 407.0 | 198.9 | 208.1 | 15 | 41 | 19.333 |
| F-3 | 360.0 | 160.0 | 200.0 | 15 | 39 | 20.040 | 358.9 | 154.1 | 204.8 | 14 | 41 | 10.197 | 395.6 | 197.1 | 198.5 | 15 | 40 | 14.644 |
| F-4 | 373.0 | 168.3 | 204.7 | 15 | 39 | 14.181 | 368.0 | 160.0 | 208.0 | 15 | 40 | 5.632 | 424.7 | 218.9 | 205.8 | 15 | 40 | 18.300 |
| F-5 | 369.2 | 162.4 | 206.8 | 14 | 41 | 31.731 | 371.2 | 162.4 | 208.8 | 14 | 41 | 10.06 | 417.2 | 214.1 | 203.1 | 15 | 39 | 14.889 |
| F-6 | 361.8 | 154.1 | 207.7 | 14 | 38 | 46.113 | 368.4 | 148.3 | 220.1 | 13 | 42 | 14.403 | 417.6 | 212.3 | 205.3 | 15 | 39 | 15.201 |
| F-7 | 386.6 | 168.3 | 218.3 | 15 | 42 | 13.736 | 382.0 | 160.0 | 222.0 | 15 | 43 | 5.619 | 436.0 | 217.7 | 218.3 | 15 | 43 | 18.313 |
| F-8 | 378.3 | 154.2 | 224.1 | 14 | 44 | 33.654 | 381.3 | 154.1 | 227.2 | 14 | 43 | 11.136 | 453.6 | 226.7 | 226.9 | 15 | 43 | 21.351 |
| F-9 | 381.5 | 160.0 | 221.5 | 15 | 44 | 13.708 | 383.4 | 160.0 | 223.4 | 15 | 44 | 5.756 | 381.5 | 160.0 | 221.5 | 15 | 44 | 20.127 |
| F-10 | 369.7 | 160.0 | 209.7 | 15 | 39 | 13.424 | 377.7 | 154.1 | 223.6 | 14 | 41 | 10.260 | 432.0 | 222.4 | 209.6 | 15 | 38 | 15.306 |
| F mean | 373.7 | 160.7 | 213.0 | 15 | 42 | 22.102 | 384.0 | 165.5 | 218.5 | 15 | 42 | 10.472 | 417.3 | 205.6 | 211.7 | 15 | 41 | 17.885 |
| G-1 | 480.1 | 234.1 | 246.0 | 21 | 46 | 70.449 | 492.3 | 242.4 | 249.9 | 21 | 47 | 22.865 | 510.3 | 273.0 | 237.3 | 23 | 46 | 23.482 |
| G-2 | 501.0 | 254.1 | 246.9 | 24 | 47 | 16.390 | 510.5 | 254.1 | 256.4 | 24 | 46 | 9.337 | 580.2 | 334.2 | 246.0 | 24 | 46 | 35.149 |
| G-3 | 450.2 | 232.4 | 217.8 | 21 | 45 | 102.881 | 458.3 | 233.0 | 225.3 | 19 | 45 | 40.653 | 503.3 | 294.8 | 208.5 | 24 | 45 | 24.259 |
| G-4 | 483.9 | 230.7 | 253.2 | 20 | 49 | 207.618 | 490.3 | 224.9 | 265.5 | 19 | 51 | 42.464 | 554.6 | 314.0 | 240.6 | 24 | 47 | 32.429 |
| G-5 | 508.4 | 250.7 | 257.7 | 22 | 48 | 40.781 | 508.6 | 250.7 | 257.9 | 22 | 49 | 16.861 | 587.9 | 341.9 | 246.0 | 23 | 46 | 16.502 |
| G-6 | 475.2 | 222.4 | 252.8 | 20 | 47 | 113.370 | 480.6 | 228.3 | 252.3 | 20 | 47 | 33.637 | 523.4 | 274.3 | 249.1 | 23 | 46 | 36.320 |
| G-7 | 445.1 | 228.3 | 216.8 | 21 | 43 | 43.609 | 455.9 | 236.6 | 219.3 | 21 | 44 | 16.189 | 490.8 | 276.6 | 214.2 | 22 | 42 | 32.231 |
| G-8 | 508.2 | 270.7 | 237.5 | 24 | 46 | 35.030 | 507.5 | 258.9 | 248.6 | 22 | 49 | 25.679 | 545.1 | 308.9 | 236.2 | 24 | 45 | 27.257 |
| G-9 | 487.6 | 248.3 | 239.3 | 23 | 46 | 69.989 | 526.8 | 263.7 | 263.1 | 20 | 53 | 38.790 | 544.5 | 310.7 | 233.8 | 24 | 45 | 17.224 |
| G-10 | 468.4 | 242.4 | 226.0 | 22 | 43 | 56.276 | 479.6 | 242.4 | 237.2 | 21 | 45 | 25.997 | 551.3 | 326.0 | 225.3 | 23 | 44 | 27.263 |
| G mean | 480.8 | 241.4 | 239.4 | 22 | 46 | 75.639 | 491.0 | 243.5 | 247.5 | 21 | 48 | 27.247 | 539.1 | 305.4 | 233.7 | 23 | 45 | 27.211 |

$C_{Total}$: Total cost $C_V$: Vehicle cost $C_D$: Drone cost $\eta$: Number of vehicle stops $\acute{\eta}$: Number of drone dispatches T: Execution time.

stations, the average execution times jumped to 75.639, 27.247, and 27.211 s, respectively. Second, the execution times of the VDH and DDH are less than that of the HCWH. Computing the multimodal savings at each iteration for the HCWH increases the required execution time for that heuristic. The execution time generally increases for HCWH and VDH in problem instances in which they continue to examine the possibility of eliminating more stations from the vehicle route. In problem instances in which customers are concentrated around a fewer number of stations and/or can be served by dispatching drones from multiple stations, they tend to examine the possibility of eliminating more stations, which increases its execution time. For example, as shown in Table 4, problem instances G-4 and G-6 recorded the highest execution times for the HCWH, and had vehicle routes with fewer stations (20 stations).

*6.3. Mothership versus vehicle-only operation*

In this set of experiments, we evaluate the potential cost savings associated with using the mothership system rather than depending only on the vehicle, as is in the current practice. Two scenarios are compared in this set of experiments. In the first scenario, two drones were dispatched and collected from one vehicle to serve all customers. The HCWH is used to obtain the solution for all test cases that adopt the mothership system. In the second scenario, one vehicle with no drones was used to serve all customers. An optimal solution (Applegate et al., 2008) and CW algorithm-based solution (Clarke and Wright, 1964) that includes all customers are obtained and used to benchmark the effectiveness of the mothership system. Comparing the mothership system with the optimal solution provides a real evaluation of how beneficial the introduction of drones may be. The comparison with the CW solution allows the mothership system and the vehicle-only system to be compared when their solutions are obtained using the same technique. When constructing the vehicle-only route, all customers are assumed to be accessible by the vehicle, and there assumed to be a direct link between any two customers. Networks B to G described above are used to compare these two scenarios. In addition, drone/ vehicle cost ratios that range from 1:2 to 1:50 are considered. Tables 5 and 6 give the results for the network instances with 50 and 100 customers, respectively. The tables give the operation cost ratios between the mothership and the vehicle-only solutions obtained using the optimal TSP solution ($\rho_{Optimal}$) and the CW algorithm ($\rho_{CW}$). The values of $\rho_{Optimal}$ and $\rho_{CW}$ indicate the effectiveness of the mothership system. If their values is below one, the solution of the mothership system is better than the vehicle-only system. Otherwise, the solution found by solving the TSP is more cost-effective.

**Table 5**

Impact of different cost-ratio for 50 customer instances.

| Cost ratio | Network B | | Network C | | Network D | |
|---|---|---|---|---|---|---|
| Drone: Vehicle | $\rho_{Optimal}$ | $\rho_{CW}$ | $\rho_{Optimal}$ | $\rho_{CW}$ | $\rho_{Optimal}$ | $\rho_{CW}$ |
| 1:2 | 1.66 | 1.66 | 1.35 | 1.31 | 1.34 | 1.26 |
| 1:5 | 1.09 | 1.09 | 0.98 | 0.95 | 1.02 | 0.96 |
| 1:10 | 0.90 | 0.90 | 0.83 | 0.80 | 0.92 | 0.86 |
| 1:25 | 0.79 | 0.79 | 0.78 | 0.75 | 0.85 | 0.80 |
| 1:50 | 0.75 | 0.75 | 0.75 | 0.73 | 0.83 | 0.78 |

$\rho_{Optimal}$: Optimal traveling salesman solution $\rho_{cw}$: Vehicle routing solution obtained using the CW algorithm

$\rho_{Optimal} \& \rho_{cw} < 1$: The mothership system is more cost effective than the vehicle-only system.

**Table 6**

Impact of different cost-ratio for 100 customer instances.

| Cost ratio | Network E | | Network F | | Network G | |
|---|---|---|---|---|---|---|
| Drone: vehicle | $\rho_{Optimal}$ | $\rho_{CW}$ | $\rho_{Optimal}$ | $\rho_{CW}$ | $\rho_{Optimal}$ | $\rho_{CW}$ |
| 1:2 | 1.45 | 1.41 | 1.37 | 1.32 | 1.40 | 1.32 |
| 1:5 | 0.89 | 0.86 | 0.89 | 0.86 | 0.99 | 0.94 |
| 1:10 | 0.70 | 0.68 | 0.73 | 0.70 | 0.85 | 0.80 |
| 1:25 | 0.59 | 0.57 | 0.64 | 0.61 | 0.77 | 0.72 |
| 1:50 | 0.55 | 0.53 | 0.61 | 0.58 | 0.73 | 0.69 |

$\rho_{Optimal}$: Optimal traveling salesman solution $\rho_{cw}$: Vehicle routing solution obtained using the CW algorithm

$\rho_{Optimal} \& \rho_{cw} < 1$: The mothership system is more cost effective than the vehicle-only system.

As shown in the tables, the mothership system is generally more cost effective than the vehicle-only system, especially when the drone's operation cost is significantly less than the vehicle cost. For example, when the drone operation cost is only half the vehicle operation cost, the vehicle-only scenario outperforms the mothership system under the assumption that the vehicle has access to all customers through direct links. As the drone operation cost decreases compared to the vehicle operation cost, the mothership system is shown to significantly outperform the vehicle-only scenario. For example, considering a drone-vehicle cost ratio of 1:25 and comparing with the CW vehicle routing solution, cost savings of 20% and 28% are recorded for network D with 50 customers and network G with 100 customers, respectively. These cost saving percentages are recorded at 15% and 23% for the same drone-vehicle cost ratio when the optimal vehicle route is obtained for the vehicle-only scenario.

Another interesting observation is related to the pattern by which the operation cost of the mothership system improves as the drone operation cost decreases as compared to that of the vehicle. For example, considering network F, $\rho_{Optimal}$ decreases by 9% when the drone-vehicle operation cost ratio changes from 1:10 to 1:25. This ratio decreases by only 3% when the drone-vehicle operation cost ratio changes from 1:25 to 1:50. Thus, it is worth investing to reduce the drone-vehicle cost ratio from 1:10 to 1:25 as it yields significant savings in the operation cost of the mothership system. Additional investment to further reduce the drone cost does not yield the same level of overall cost improvement. These results are comparable with the savings results reported in Ha et al. (2018), in which one drone is used in the form of flying side-kick delivery system.

### 6.4. Effect of number of drones carried by the vehicle

In all of the experiments described above, the vehicle is assumed to carry two drones onboard. In this set of experiments, we examine the effect of the number of drones on overall network performance. Scenarios with a vehicle with one, two, and three drones are considered. The vehicle's operation cost is assumed to be twice the drones' cost. The results of this set of experiments is given in Table 7.

**Table 7**

The performance of the heuristics considering different number of drones.

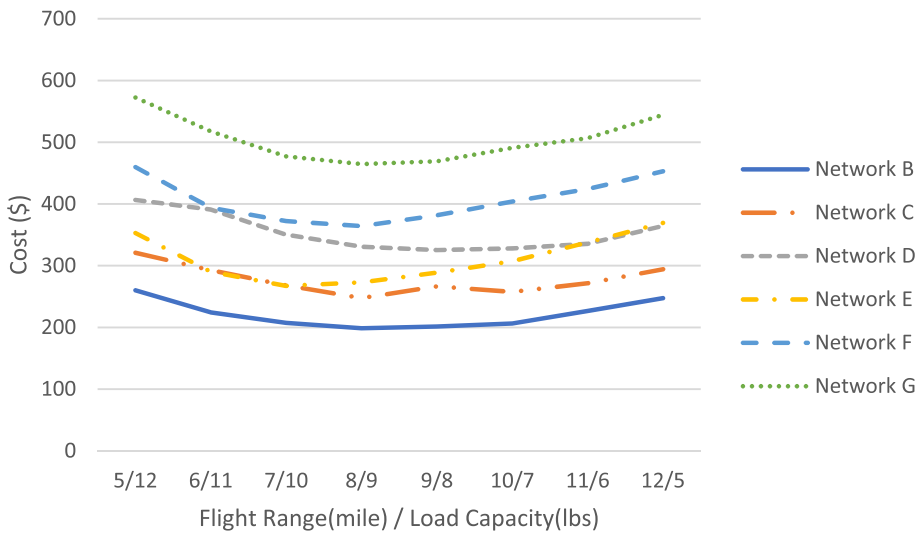| Instance | One drone | | | Two drones | | | Three drones | | |
|---|---|---|---|---|---|---|---|---|---|
| | HCWH | VDH | DDH | HCWH | VDH | DDH | HCWH | VDH | DDH |
| B | 209.0 | 209.0 | 240.2 | 207.4 | 207.4 | 232.6 | 206.4 | 206.4 | 232.6 |
| C | 271.1 | 274.4 | 308.9 | 269.3 | 273.3 | 303.2 | 269.3 | 272.3 | 311.3 |
| D | 343.7 | 345.2 | 405.4 | 343.3 | 348.8 | 404.5 | 343.5 | 348.8 | 419.0 |
| E | 272.1 | 272.1 | 269.7 | 267.4 | 268.7 | 298.9 | 266.7 | 267.6 | 301.6 |
| F | 372.1 | 373.3 | 427.6 | 372.2 | 368.8 | 403.4 | 369.4 | 368 | 399.8 |
| G | 481.7 | 491.6 | 525.4 | 480.4 | 487.0 | 531.3 | 475.3 | 483.7 | 556.8 |

**Fig. 11.** Flight range versus load capacity.

The results indicate that the effect of increasing the number of drones on the total network cost is not the same across the three heuristics. Increasing the number of drones resulted in a cost reduction when the HCWH and the VDH are used to solve the hybrid routing problem. On the contrary, the cost of the DDH solution increases with an increase in the number of drones. For example, for network G, the HCWH resulted in a cost of $481.70 when one drone is used. This cost decreased to $475.30 for the three-drone scenario. A similar pattern is observed for the VDH. For the DDH, the network cost was recorded at $525.40, $531.30, and $556.80 for one, two, and three drones, respectively. Using limited number of drones constrains the structure of the drone's routes in order to be able to visit all customers. The drones are forced to make more returns to their dispatching stations. However, as more drones are included, more efficient drone routes could be constructed which, reduces the total cost as observed in the results of the HCWH and VDH. For the DDH, the drone routes are further optimized in a greedy way, which causes significant inefficiencies to the vehicle route as more stops are required for the drones. The increase in the cost of the vehicle route leads to an increase in the total cost of the network as reported above.

*6.5. Trade-off between flight range and load carrying capacity*

Carrying a heavier load requires a drone to have a large battery and strong drone frame, which in turn adds weight to the drone and shortens its range. Thus, planning an efficient vehicle-drone delivery service requires examining the trade-off between the drones' flight range and load carrying capacity (Flynt, 2017). For that purpose, a set of experiments are conducted in which drones with different flight ranges and load carrying capacities are considered. The total network operation cost is recorded for several networks.

As illustrated in Fig. 11, using drones with a small flight range (the left side of the x-axis), irrespective of the load carrying capacity, resulted in networks with high operation costs. Similarly, using drones with limited load carrying capacity (the right side of the x-axis), irrespective of the flight range, increased the total operation cost. For example, an operation cost of $573.00 is recorded for network G for the scenario in which drones with a flight range of 5.0 miles and a load carrying capacity of 12.0 lbs. are used. Increasing the drone's flight range to 12.0 miles and reducing their load carrying capacity to 5.0 lbs. resulted in an operation cost of $544.00. The results in the figure show that there is an optimal combination of the drone's flight range and load carrying capacity that minimizes the total operation cost of the network. With the exception of networks E and D, the least operation cost is recorded for drones with a flight range of 8.0 miles and a load carrying capacity of 9.0 lbs. For network E, which has the highest customer density (1.0 customer/mile$^2$), the least operation cost is recorded for drones with a relatively higher load carrying capacity. A cost of $267.00 is recorded for drones with flight range of 7.0 miles and load carrying capacity of 10 lbs. On the other hand, for network D, which has a low customer density of 0.10 customer/mile$^2$, drones with a relatively long flight range (9.0 miles) are required to efficiently serve the sparsely distributed customers.

**7. Conclusion**

The vehicle-drone "mothership" system was recently conceptualized to provide efficient pick-up and delivery services. Drones could be mounted on the vehicles and dispatched from pre-specified stations to deliver and pick-up products to/from a set of customers distributed in a given service area. This paper presents a model and efficient solution methodology for the HVDRP for pick-up and delivery services. A mathematical formulation in the form of a mixed integer program is developed which solves for the optimal vehicle and drone routes to serve all customers such that the total cost of the pick-up and delivery operation is minimized. The formulation captures the vehicle-drone routing interactions and considers the drone's operational constraints including flight range and load carrying capacity limitations. A novel

solution methodology that extends the classic Clarke and Wright algorithm is developed to solve the HVDRP, namely the HCWH. The heuristic takes into consideration the cost savings resulting from connecting stops in the vehicle route and connecting customers in the drone routes that are dispatched and collected at these stops. The performance of the HCWH is benchmarked against the VDH and the DDH. In the VDH, an efficient vehicle route is first obtained, and the drones are then routed considering the dispatching and collection stops specified in the vehicle route. The drone-driven routing heuristic determines the drone routes and specifies optimal locations for their dispatching and collection. The vehicle is then routed to visit these stops.

The developed heuristics are shown to produce high quality solutions that are comparable to the exact optimal solution for small problem instances. The heuristics are also able to solve large problem instances in shorter execution times. While the VDH and the DDH focus on optimizing the cost of one mode only, the HCWH is shown to outperform these two heuristics in terms of minimizing the cost of the entire multimodal network. The results also show the value of adopting the mothership system. Compared to a scenario in which the vehicle is used to visit all customers, the amount of cost reduction increases as the drone's operation cost decreases. Finally, the network operation cost is shown to be minimum when the used drones are balanced in terms of their flight range and load carrying capacity. Generally, service areas characterized by high customer density require drones with large load carrying capacity. For service areas with sparse customers, drones with long flight range are more suitable. Several extensions are considered for this research work. First, effort is underway to extend the formulation and the solution methodology for the multi-vehicle mothership system in which multiple vehicles are used instead of one vehicle. Second, the framework could be extended to solve the real-time version of the problem in which on-demand pick-up and delivery requests are considered. We also consider extending this research by comparing the performance of the heuristics presented in this paper against those of meta-heuristic approaches including a genetic algorithm (Baker and Ayechew, 2003) and a tabu search algorithm (Gendreau et al., 1994). The effort could also be extended to improve the mathematical formulation of the MIP to enhance its execution time. Finally, we are exploring applying this model to other emerging problem domains such as drone/flying taxis and emergency response services (Lei et al., 2015).

## Acknowledgement

## Appendix A. Deterministic HCWH versus stochastic HCWH

A stochastic version of the deterministic HCWH is implemented, the SHCWH. The SHCWH starts by randomizing the descending-ordered savings list. The first $E$ elements in the savings list are selected and randomly rearranged. The process is repeated for the next $E$ elements until the entire list is randomized. The problem is again solved using the randomized savings list. If a better solution is

**Table A1**
Comparison between the HCWH and the SHCWH.

| Instance | HCWH | | | |
|---|---|---|---|---|
| | $C_{Total}$ ($) | $T$ (seconds) | $\Delta$ (%) | Time ratio |
| G-1 | 480.1 | 81.767 | – | – |
| G-2 | 501.0 | 23.867 | – | – |
| G-3 | 450.2 | 110.063 | – | – |
| Instance | SHCWH $n = 100$ | | | |
| | $C_{Total}$ ($) | $T$ (seconds) | $\Delta$ (%) | Time ratio |
| G-1 | 476.1 | 1387.807 | 0.83 | 16.97 |
| G-2 | 501.0 | 701.058 | 0.00 | 29.37 |
| G-3 | 445.5 | 2626.680 | 1.04 | 23.87 |
| Instance | SHCWH $n = 300$ | | | |
| | $C_{Total}$ ($) | $T$ (seconds) | $\Delta$ (%) | Time ratio |
| G-1 | 476.1 | 5287.226 | 0.83 | 64.66 |
| G-2 | 501.0 | 2068.865 | 0.00 | 86.68 |
| G-3 | 445.5 | 8325.795 | 1.04 | 75.65 |
| Instance | SHCWH $n = 500$ | | | |
| | $C_{Total}$ ($) | $T$ (seconds) | $\Delta$ (%) | Time ratio |
| G-1 | 475.5 | 9858.278 | 0.96 | 120.565 |
| G-2 | 501.0 | 3232.943 | 0.00 | 135.456 |
| G-3 | 445.5 | 11215.715 | 1.04 | 101.90 |

found, the new savings list is updated and randomly rearranged as described above. Otherwise, the current savings list is again randomized and used to determine a new solution. If no better solution is found for a pre-specified number of iterations, $n$, the heuristic terminates, producing the best solution in all iterations. We compared the performance of the HCWH to that of the SHCWH. The two heuristics were used to obtain the solution for three different instances of network G. The number of iterations, $n$, considered for the SHCWH are 100, 300 and 500, and $E$ is randomly generated such that it ranges from zero to six, respectively. The results gives the percentage improvement, $\Delta$, in the total network cost and the magnitude by which the execution time increased (as multiples of the HCWH's execution time), as compared to those of the deterministic HCWH. As presented in Table A1, the SHCWH is able to achieve a slight solution improvement of about 1.0% for instances G-1 and G-3. This improvement does not seem to increase with the increase in the number of iterations. The slight improvement in the solution is associated with a significant increase in the execution time. For example, for the 100 iteration case, the SHCWH's execution time for G-3 is recorded to be about 24 times of that recorded for HCWH. No improvement is recorded for instance G-2.

# References

Agatz, N., Bouman, P., Marie, S., 2016. Optimization approaches for the traveling salesman problem with drone. Transportation Sci. 1–17.

Applegate, D., Bixby, R., Chvatal, V., Cook, W., 2008. Concorde TSP solver.

Avellar, G., Pereira, G., Pimenta, L., Iscold, P., 2015. Multi-uav routing for area coverage and remote sensing with minimum time. Sensors 15 (11), 27783–27803.

Baker, B.M., Ayechew, M.A., 2003. A genetic algorithm for the vehicle routing problem. Comput. Oper. Res. 30 (5), 787–800.

Balasingam, M., 2017. Drones in medicine—The rise of the machines. Int. J. Clin. Pract. 71 (9), 1–4.

Berbeglia, G., Cordeau, J.-F., Laporte, G., 2010. Dynamic pickup and delivery problems. Eur. J. Oper. Res. 202 (1), 8–15.

Borcinova, Z., 2017. Two models of the capacitated vehicle routing problem. Croatian Operational Res. Rev. 8 (2), 463–469.

Bouman, P., Agatz, N., Schmidt, M., 2017. Dynamic programming approaches for the traveling salesman problem with drone. ERIM Res. Paper Series.

Braekers, K., Ramaekers, K., Nieuwenhuysec, I.V., 2014. The vehicle routing problem: State of the art classification and review. Comput. Ind. Eng. 99, 300–313.

Chao, M., 2002. A tabu search method for the truck and trailer routing problem. Comput. Oper. Res. 29 (1), 33–51.

Chowdhury, S., Emelogua, A., Marufuzzamana, M., Nurre, S.G., Bian, L., 2017. Drones for disaster response and relief operations: A continuous approximation model. Int. J. Prod. Econ. 188, 167–184.

Christofides, N., 1976. The vehicle routing problem. Revue française d'automatique, informatique, recherche opérationnelle. Recherche opérationnelle 10 (1), 55–70.

Clarke, G., Wright, J.W., 1964. Scheduling of vehicles from a central depot to a number of delivery points. Oper. Res. 12 (4), 568–581.

Clarke, R., Moses, L.B., 2014. The regulation of civilian drones' impacts on public safety. Comput. Law Security Rev. 30 (3), 263–285.

Cuda, R., Guastaroba, G., Speranza, M., 2015. A survey on two-echelon routing problems. Comput. Oper. Res. 55, 185–199.

Derigs, U., Pullmann, M., Vogel, U., 2013. Truck and trailer routing—problems, heuristics and computational experience. Comput. Oper. Res. 40 (2), 536–546.

Dorling, K., Heinrichs, J., Messier, G.G., 2016. Vehicle routing problems for drone delivery. IEEE Trans. Syst., Man Cybernetics: Syst. 47 (1), 70–85.

Eksioglu, B., Vuralb, A.V., Reismanc, A., 2009. The vehicle routing problem: A taxonomic review. Comput. Ind. Eng. 57 (4), 1472–1483.

Erdogan, S., Miller-Hooks, E., 2012. A green vehicle routing problem. Transportation Res. Part E: Logistics Transportation Rev. 48 (1), 100–114.

Fargeas, J.L., Kabamba, P., Girard, A., 2015. Cooperative surveillance and pursuit using unmanned aerial vehicles and unattended ground sensors. Sensors 15 (1), 1365–1388.

Floreano, D., Wood, R.J., 2015. Science, technology and the future of small autonomous drones. Nature 521 (7553), 460–466.

Flynt, J., 2017. How Much Weight Can a Drone Carry? Retrieved July 24, 2018 < http://3dinsider.com/drone-payload/ > .

Fukasawa, Ricardo, Longo, Humberto, Lysgaard, Jens, de Aragão, Marcus Poggi, Reis, Marcelo, Uchoa, Eduardo, Werneck, Renato F., 2006. Robust branch-and-cut-and-price for the capacitated vehicle routing problem. Math. Programming 106 (3), 491–511.

Gendreau, M., Hertz, A., Laporte, G., 1994. A tabu search heuristic for the vehicle routing problem. Manage. Sci. 40 (10), 1276–1290.

Getzin, S., Wiegand, K., Schöning, I., 2012. Assessing biodiversity in forests using very high-resolution images and unmanned aerial vehicles. Methods Ecol. Evol. 3 (2), 397–404.

Golden, B., Raghavan, S., Wasil, E., 2008. The vehicle routing problem: latest advances and new challenges. Operations Research/Computer Science Interface Series, vol 43 Springer.

Govindan, K., Jafarian, A., Khodaverdi, R., Devika, K., 2014. Two-echelon multiple-vehicle location–routing problem with time windows for optimization of sustainable supply chain network of perishable food. Int. J. Prod. Econ. 152, 9–28.

Grochlsky, B., Keller, J., Kumar, V., Pappas, G., 2006. Cooperative air and ground surveillance. IEEE Rob. Autom. Mag. 13 (3), 1070–9932.

Ha, Q.M., Deville, Y., Pham, Q.D., Hà, M.H., 2018. On the min-cost traveling salesman problem with drone. Transportation Res. Part C: Emerging Technol. 86, 597–621.

Ham, A.M., 2018. Integrated scheduling of m-truck, m-drone, and m-depot constrained by time-window, drop-pickup, and m-visit using constraint programming. Transportation Res. Part C: Emerging Technol. 91, 1–14.

Hiermann, G., Puchinger, J., Ropke, S., Hart, R.F., 2016. The electric fleet size and mix vehicle routing problem with time windows and recharging stations. Eur. J. Oper. Res. 252 (3), 995–1018.

Jeong, H.Y., Lee, S., Song, B.D., 2019. Truck-drone hybrid delivery routing: payload-energy dependency and no-fly zones. Int. J. Prod. Economics In Press.

Kim, S., Moon, I., 2019. Traveling salesman problem with a drone station. IEEE Trans. Syst., Man, Cybernetics: Syst. 49 (1), 42–52.

Kim, S.J., Lim, G.J., Cho, J., Côté, M.J., 2017. Drone-aided healthcare services for patients with chronic diseases in rural areas. Intell. Robotic Syst. 88 (1), 163–180.

Kunze, O., 2016. Replicators, ground drones and crowd logistics a vision of urban logistics in the year 2030. Transp. Res. Procedia 19, 286–299.

Lei, S., Hua, Y., Xufeng, Y., Cong, M., Jun, H., 2015. A study of instability in a miniature flying-wing aircraft in high-speed taxi. Chin. J. Aeronaut. 28 (3), 749–756.

Lin, C., 2011. A vehicle routing problem with pickup and delivery time windows, and coordination of transportable resources. Comput. Oper. Res. 1596–1609.

Lin, S.W., Yu, Vincent F., Chou, S.-Y., 2009. Solving the truck and trailer routing problem based on a simulated annealing heuristic. Comput. Oper. Res. 36 (5), 1683–1692.

Lockridge, D., 2017. The big and small of last mile delivery. Retrieved July 24, 2018 < http://www.truckinginfo.com/channel/fleet-management/article/story/2017/04/the-big-and-small-of-the-last-mile-delivery.aspx > .

McFarland, M., 2016. This Mercedes-Benz van will carry a fleet of delivery robots. Retrieved July 24, 2018 < http://money.cnn.com/2016/09/07/technology/starship-robot-mercedes-benz/index.html > .

McFarland, M., 2017. UPS drivers may tag team deliveries with drones. Retrieved July 24, 2018 < https://money.cnn.com/2017/02/21/technology/ups-drone-delivery/index.html > .

Menouar, H., Guvenc, I., Akkaya, K., Uluagac, A.S., Kadri, A., Tuncer, A., 2017. UAV-enabled intelligent transportation systems for the smart city: applications and challenges. IEEE Commun. Mag. 55 (3), 22–28.

Merwaday, A., Guvenc, I., 2015. UAV assisted heterogeneous networks for public safety communications. In: 2015 IEEE Wireless Communications and Networking Conference Workshops (WCNCW). IEEE, New Orleans, LA, USA, pp. 329–334.

Murray, C., Chu, A., 2015. The flying sidekick traveling salesman problem: Optimization of drone-assisted parcel delivery. Transportation Part C: Emerging Technol.

    54, 86–109.

Nguyen, V.P., Prins, C., Prodhon, C., 2012. Solving the two-echelon location routing problem by a GRASP reinforced by a learning process and path relinking. Eur. J. Oper. Res. 216 (1), 113–126.

Paust, J.J., 2010. Self-defense targetings of non-state actors and permissibility of U.S. use of drones in Pakistan. Transnational Law & Policy 19 (2), 237–282.

Petersen, R., 2016. Rethinking last-mile logistics: deploying swarms of drones with self-driving trucks. Retrieved July 24, 2018 < https://www.flexport.com/blog/deploying-drones-self-driving-trucks/ > .

Poikonen, S., Wang, X., Golden, B., 2017. The vehicle routing problem with drones: Extended models and connections. Networks 70 (1), 34–43.

PYMNTS, 2016. MERCHANT INNOVATIONIs Drone Delivery Economically Feasible, Practical? Retrieved July 24, 2018 < https://www.pymnts.com/news/merchant-innovation/2016/economics-drone-delivery/ > .

Rash, W., 2017. UPS tests delivery trucks equipped with drones as efficiency booster. Retrieved July 24, 2018 < http://www.eweek.com/mobile/ups-tests-delivery-trucks-equipped-with-drones-as-efficiency-booster > .

Rose, C., 2013. Amazon's Jeff Bezos Looks to the Future. Retrieved July 24, 2018 < https://www.cbsnews.com/news/amazons-jeff-bezos-looks-to-the-future/ > .

Schneider, M., Stenger, A., Goeke, D., 2014. The electric vehicle-routing problem with time windows and recharging stations. Transportation Sci. 48 (4), 500–520.

Schneiderman, R., 2012. Unmanned drones are flying high in the military/aerospace sector [special reports]. IEEE Signal Process Mag. 29 (1), 8–11.

Shetty, V., Sudit, M., Nagi, R., 2008. Priority-based assignment and routing of a fleet of unmanned combat aerial. Comput. Oper. Res. 35, 1813–1828.

Thiels, C., Aho, J., Zietlow, S., Jenkins, D., 2015. Use of unmanned aerial vehicles for medical product transport. Air Med. J. 34 (2), 104–108.

Troudi, A., Addouche, S.-A., Dellagi, S., Mhamed, A.E., 2017. Logistics support approach for drone delivery fleet. In: International Conference on Smart Cities. Springer, Cham, Malaga, Spain, pp. 86–96.

Vattapparamban, E., Güvenç, İ., Yurekli, A.İ., Akkaya, K., Uluağaç, S., 2016. Drones for smart cities: Issues in cybersecurity, privacy, and public safety. In: 2016 International Wireless Communications and Mobile Computing Conference (IWCMC). IEEE, Paphos, Cyprus, pp. 216–221.

Villegas, J.G., Prins, C., Prodhon, C., L.Medaglia, A., Velascod, N., 2013. A matheuristic for the truck and trailer routing problem. Eur. J. Oper. Res. 230 (2), 231–244.

Wang, X., Poikonen, S., Golden, B., 2017. The vehicle routing problem with drones: Several worst-case results. Optimization Lett. 11 (4), 679–697.

Xiao, Y., Zhao, Q., Kaku, I., Xu, Y., 2012. Development of a fuel consumption optimization model for the capacitated vehicle routing problem. Comput. Oper. Res. 39 (7), 1419–1431.